

# $R_b$ and New Physics: A Comprehensive Analysis

P. Bamert<sup>a</sup>, C.P. Burgess<sup>a</sup>, J.M. Cline<sup>a</sup>,  
D. London<sup>a,b</sup> and E. Nardi<sup>c</sup>

<sup>a</sup> *Physics Department, McGill University  
3600 University St., Montréal, Québec, Canada, H3A 2T8*

<sup>b</sup> *Laboratoire de Physique Nucléaire, Université de Montréal  
C.P. 6128, succ. centre-ville, Montréal, Québec, Canada, H3C 3J7*

<sup>c</sup> *Department of Particle Physics  
Weizmann Institute of Science, Rehovot 76100, Israel*

## Abstract

We survey the implications for new physics of the discrepancy between the LEP measurement of  $R_b$  and its Standard Model prediction. Two broad classes of models are considered: (i) those in which new  $Z\bar{b}b$  couplings arise at tree level, through  $Z$  or  $b$ -quark mixing with new particles, and (ii) those in which new scalars and fermions alter the  $Z\bar{b}b$  vertex at one loop. We keep our analysis as general as possible in order to systematically determine what kinds of features can produce corrections to  $R_b$  of the right sign and magnitude. We are able to identify several successful mechanisms, which include most of those which have been recently been proposed in the literature, as well as some earlier proposals (*e.g.* supersymmetric models). By seeing how such models appear as special cases of our general treatment we are able to shed light on the reason for, and the robustness of, their ability to explain  $R_b$ .

## 1. Introduction

The Standard Model (SM) of electroweak interactions has been tested and confirmed with unprecedented precision over the past few years using measurements of  $e^+e^-$  scattering at the  $Z$  resonance at LEP [1] and SLC [2]. A particularly striking example of the impressive SM synthesis of the data came with the discovery, at CDF and D0 [3], of the top quark with a mass which is in excellent agreement with the value implied by the measurements at LEP.

The biggest — and only statistically important — fly to be found so far in the proverbial SM ointment is the experimental surplus of bottom quarks produced in  $Z$  decays, relative to the SM prediction. With the analysis of the 1994 data as described at last summer's conferences [1][2], this discrepancy has become almost a  $4\sigma$  deviation between experiment and SM theory. The numbers are:

$$R_b \equiv \Gamma_b/\Gamma_{\text{had}} = 0.2219 \pm 0.0017, \quad \text{while} \quad R_b(\text{SM}) = 0.2156. \quad (1)$$

The SM prediction assumes a top mass of  $m_t = 180$  GeV and the strong coupling constant  $\alpha_s(M_Z) = 0.123$ , as is obtained by optimizing the fit to the data.

There are other measurements which differ from their SM predictions at the  $\geq 2\sigma$  level:  $R_c$  ( $2.5\sigma$ ),  $A_{FB}^0(\tau)$  ( $2.0\sigma$ ), and the inconsistency ( $2.4\sigma$ ) between  $A_e^0$  as measured at LEP with that obtained from  $A_{LR}^0$  as determined at SLC [2]. In fact, since the  $R_c$  and  $R_b$  measurements are correlated, and because they were announced together, some authors refer to this as the “ $R_b$ - $R_c$  crisis.” One of the points we wish to make in this paper is that there is no  $R_c$  crisis. If the  $R_b$  discrepancy can be resolved by the addition of new physics, one then obtains an acceptable fit to the data. In other words,  $R_c$ , as well as  $A_{FB}^0(\tau)$  and  $A_{LR}^0$ , can reasonably be viewed simply as statistical fluctuations.

On the other hand, it is difficult to treat the measured value of  $R_b$  as a statistical fluctuation. Indeed, largely because of  $R_b$ , the data at face value now *exclude* the SM at the 98.8% confidence level. If we suppose that this disagreement is not an experimental artifact, then the burning question is: What Does It Mean?

Our main intention in this paper is to survey a broad class of models to determine what kinds of new physics can bring theory back into agreement with experiment. Since  $R_b$  is the main culprit we focus on explaining both its sign and magnitude. This is nontrivial, but not impossible to do, given that the discrepancy is roughly the same size as, though in the opposite direction to, the large  $m_t$ -dependent SM radiative correction. The result is therefore just within the reach of one-loop perturbation theory.

Our purpose is to survey the theoretical possibilities within a reasonably broad framework, and we therefore keep our analysis quite general, rather than focusing on individual models. This approach has the virtue of exhibiting features that are generic to sundry explanations of the  $Z \rightarrow b\bar{b}$  width, and many of the proposals of the literature emerge as special cases of the alternatives which we consider.

In the end we find a number of possible explanations of the effect, each of which would have its own potential signature in future experiments. These divide roughly into two categories: those which introduce new physics into  $R_b$  at tree level, and those which do so starting at the one-loop level.

The possibilities are explored in detail in the remainder of the article, which has the following organization. The next section discusses why  $R_b$  is the only statistically significant discrepancy between theory and experiment, and summarizes the kinds of interactions to which the data points. This is followed by several sections, each of which examines a different class of models. Section 3 studies the tree-level possibilities, consisting of models in which the  $Z$  boson or the  $b$  quark mixes with a hitherto undiscovered particle. We find several viable models, some of which imply comparatively large modifications to the right-handed  $b$ -quark neutral-current couplings. Sections 4 and 5 then consider loop contributions to  $R_b$ . Section 4 concerns modifications to the  $t$ -quark sector of the SM. Although we find that we can reduce the discrepancy in  $R_b$  to  $\sim 2\sigma$ , we do not regard this as sufficient to claim success for models of this type. Section 5 then considers the general form for loop-level modifications of the  $Z\bar{b}b$  vertex which arise from models with new scalars and fermions. The general results are then applied to a number of illustrative examples. We are able to see why simple models, like multi-Higgs doublet and Zee-type models fail to reproduce the data, as well as to examine the robustness of the difficulties of a supersymmetric explanation of  $R_b$ . Finally, our general expressions guide us to some examples which *do* make experimentally successful predictions. Section 6 discusses some future experimental tests of various explanations of the  $R_b$  problem. Our conclusions are summarized in section 7.

## 2. The Data Speaks

Taken at face value, the current LEP/SLC data excludes the SM at the 98.8% confidence level. It is natural to ask what new physics would be required to reconcile theory and experiment in the event that this disagreement survives further experimental scrutiny. Before digging through one's theoretical repertoire for candidate models, it behooves the theorist first to ask which features are preferred in a successful explanation of the data.

An efficient way to do so is to specialize to the case where all new particles are heavy enough to influence  $Z$ -pole observables primarily through their lowest-dimension interactions in an effective lagrangian. Then the various effective couplings may be fit to the data, allowing a quantitative statistical comparison of which ones give the best fit. Although not all of the scenarios which we shall describe involve only heavy particles, many of them do and the conclusions we draw using an effective lagrangian often have a much wider applicability than one might at first assume. Applications of this type of analysis to earlier data [4][5] have been recently updated to include last summer's data [6], and the purpose of this section is to summarize the results that were found.

There are two main types of effective interactions which play an important role in the analysis of  $Z$ -resonance physics, and we pause first to enumerate briefly what these are. (For more details see Ref. [4].) The first kind of interaction consists of the lowest-dimension deviations to the electroweak boson self-energies, and can be parameterized using the well-known Peskin-Takeuchi parameters  $S$  and  $T$  [7].<sup>1</sup> The second class of interactions consists of nonstandard dimension-four effective neutral-current fermion couplings, which may be defined as follows:<sup>2</sup>

$$\mathcal{L}_{\text{eff}}^{\text{nc}} = \frac{e}{s_w c_w} Z_\mu \bar{f} \gamma^\mu [(g_L^f + \delta g_L^f) \gamma_L + (g_R^f + \delta g_R^f) \gamma_R] f. \quad (2)$$

In this expression  $g_L^f$  and  $g_R^f$  denote the SM couplings, which are normalized so that  $g_L^f = I_3^f - Q^f s_w^2$  and  $g_R^f = -Q^f s_w^2$ , where  $I_3^f$  and  $Q^f$  are the third component of weak isospin and the electric charge of the corresponding fermion,  $f$ .  $s_w = \sin \theta_w$  denotes the sine of the weak mixing angle.

Fitting these effective couplings to the data leads to the following conclusions.

- (1) *What Must Be Explained:* Although the measured values for several observables depart from SM predictions at the  $2\sigma$  level and more, at the present level of experimental accuracy it is only the  $R_b$  measurement which really must be theoretically explained. After all, some  $2\sigma$  fluctuations are not surprising in any sample of twenty or more independent measurements. (Indeed, it would be disturbing, statistically speaking, if all measurements agreed with theory to within  $1\sigma$ .) This observation is reflected quantitatively in the fits of Ref. [6], for which the minimal modification which is required to accommodate the  $R_b$  measurement, namely the addition of only new effective  $Z\bar{b}b$  couplings, already raises the

---

<sup>1</sup> The third parameter,  $U$ , also appears but doesn't play a role in the  $Z$ -pole observables.

<sup>2</sup> Here we introduce a slight notation change relative to Ref. [4] in that our couplings  $\delta g_{L,R}^f$  correspond to  $\delta \hat{g}_{L,R}^f$  of Ref. [4].

confidence level of the fit to acceptable levels ( $\chi^2_{min}/\text{d.o.f.} = 15.5/11$  as compared to 27.2/13 for a SM fit). We therefore regard the evidence for other discrepancies with the SM, such as the value of  $R_c$ , as being inconclusive at present and focus instead on models which predict large enough values for  $R_b$ .

- (2) *The Significance of  $R_c$* : Since the 1995 summer conferences have highlighted the nonstandard measured values for the  $Z$  branching ratio into *both*  $c$  and  $b$  quarks, it is worth making the above point more quantitatively for the particular case of the discrepancy in  $R_c$ . This was addressed in Ref. [6] by introducing effective couplings of the  $Z$  to both  $b$  and  $c$  quarks, and testing how much better the resulting predictions fit the observations. Although the goodness of fit to  $Z$ -pole observables *does* improve somewhat (with  $\chi^2_{min}/\text{d.o.f.} = 9.8/9$ ), it does so at the expense of driving the preferred value for the strong coupling constant up to  $\alpha_s(M_Z) = 0.180 \pm 0.035$ , in disagreement at the level of  $2\sigma$  with low-energy determinations, which lie in the range  $0.112 \pm 0.003$  [8]. This change in the fit value for  $\alpha_s(M_Z)$  is driven by the experimental constraint that the total  $Z$  width not change with the addition of the new  $Z\bar{c}c$  couplings.<sup>3</sup> Once the low-energy determinations of  $\alpha_s(M_Z)$  are also included,  $\chi^2_{min}/\text{d.o.f.}$  not only drops back to the levels taken in the fit only to effective  $Z\bar{b}b$  couplings, but the best-fit prediction for  $R_c$  again moves into a roughly  $2\sigma$  discrepancy with experiment.

It is nevertheless theoretically possible to introduce new physics to account for  $R_c$  in a way which does not drive up the value of the strong coupling constant. As argued on model-independent grounds in Ref. [6], and more recently within the context of specific models [9][10], an alteration of the  $c$ -quark neutral-current couplings can be compensated for in the total  $Z$  width by also altering the neutral-current couplings of light quarks, such as the  $s$ . We put these types of models aside in the present paper, considering them to be insufficiently motivated by the experimental data.

- (3) *LH vs. RH Couplings*: The data do not yet permit a determination of whether it is preferable to modify the left-handed (LH) or right-handed (RH)  $Z\bar{b}b$  coupling. The minimum values for  $\chi^2$  found in Ref. [6] for a fit involving either LH, RH or both couplings are, respectively,  $\chi^2_{min}/\text{d.o.f.}(\text{LH}) = 17.0/12$ ,  $\chi^2_{min}/\text{d.o.f.}(\text{RH}) = 16.1/12$  or  $\chi^2_{min}/\text{d.o.f.}(\text{both}) = 15.5/11$ .

---

<sup>3</sup> Introducing effective  $b$ -quark couplings have precisely the opposite effect — since the SM prediction for  $\Gamma_b$  is low and that for  $\Gamma_c$  is high relative to observations — lowering the strong coupling constant to  $\alpha_s(M_Z)=0.103\pm0.007$ .

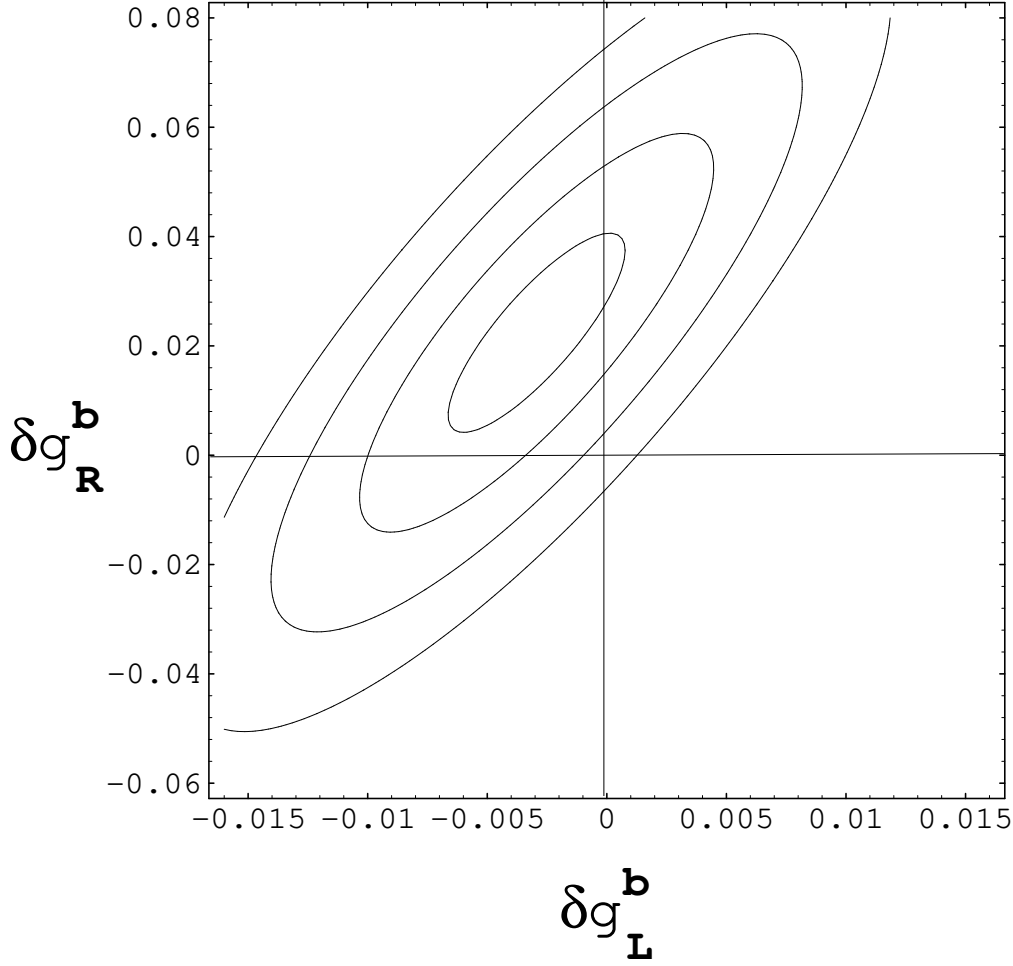


Figure 1: A fit

of the  $Z\bar{b}b$  couplings  $\delta g_{L,R}^b$  to  $Z$ -pole data from the 1995 Summer Conferences. The four solid lines respectively denote the  $1\sigma$ ,  $2\sigma$ ,  $3\sigma$ , and  $4\sigma$  error ellipsoids. The SM prediction lies at the origin,  $(0, 0)$ . This fit yields  $\alpha_s(M_Z) = 0.101 \pm 0.007$ .

- *(4) The Size Required to Explain  $R_b$ :* The analysis of Ref. [6] also indicates the size of the change in the neutral-current  $b$ -quark couplings that is required if these are to properly describe the data. The best fit values which are required are displayed in Figure 1, and are listed in Table 1. Table 1 also includes for comparison the corresponding tree-level SM couplings, as well as the largest SM one-loop vertex corrections (those which depend quadratically or logarithmically on the  $t$ -quark mass<sup>4</sup>  $m_t$ ), evaluated at  $s_w^2 = 0.23$ . For making comparisons we take  $m_t = 180$  GeV.

As we now describe, the implications of the numbers appearing in Table 1 depend on the handedness (LH *vs.* RH) of effective new-physics  $Z\bar{b}b$  couplings.

- *(4a) LH Couplings:* Table 1 shows that the required change in the LH  $Z\bar{b}b$  couplings must

---

<sup>4</sup> More precisely [11], we use  $\delta g_L^b = (\frac{\alpha_w}{16\pi})[r + 2.88 \ln r]$ , where  $r = m_t^2/M_W^2$ .

Coupling	$g(\text{SM tree})$	$\delta g(\text{SM top loop})$	$\delta g(\text{Individual Fit})$	$\delta g(\text{Fit to Both})$
$g_L^b$	-0.4230	0.0065	$-0.0067 \pm 0.0021$	$-0.0029 \pm 0.0037$
$g_R^b$	0.0770	0	$0.034 \pm 0.010$	$0.022 \pm 0.018$

**Table 1**

Required Neutral-Current  $b$ -Quark Couplings: The last two columns display the size of the effective correction to the left- and right-handed SM  $Z\bar{b}b$  couplings which best fit the data. The “individual fit” is obtained using only one effective chiral coupling in addition to the SM parameters  $m_t$  and  $\alpha_s(M_Z)$ . The “fit to both” includes both couplings. Also shown for comparison are the SM predictions for these couplings, both the tree-level contribution (“SM tree”), and the dominant  $m_t$ -dependent one-loop vertex correction, evaluated at  $s_w^2=0.23$  (“SM top loop”).

be negative and comparable in magnitude to the  $m_t$ -dependent loop corrections within the SM. The sign must be negative since the prediction for the  $Z \rightarrow b\bar{b}$  width must be increased relative to the SM result in order to agree with experiment. This requires  $\delta g_L^b$  to have the same sign as the tree-level value for  $g_L^b$ , which is negative. As we shall see, this sign limits the kinds of models which can produce the desired effect. Comparison with the SM loop contribution shows that the magnitude required for  $\delta g_L^b$  is reasonable for a one-loop calculation. Since the size of the  $m_t$ -dependent part of the SM loop is enhanced by a factor of  $m_t^2/M_W^2$ , the required new-physics effect must be *larger* than a generic electroweak loop correction.

- *(4b) RH Couplings:* Since the SM tree-level RH coupling is opposite in sign to its LH counterpart and is some five times smaller, the new-physics contribution required by the data,  $\delta g_R^b$ , is positive and comparable in size to the tree-level coupling. This makes it likely that any new-physics explanation of the data which relies on changing  $g_R^b$  must arise at tree level, rather than through loops.

- *(5) Absence of Oblique Corrections:* A final proviso is that any contribution to  $g_L^b$  or  $g_R^b$  should not be accompanied by large contributions to other physical quantities. For example, Ref. [6] finds that the best-fit values for the oblique parameters  $S$  and  $T$  are

$$\begin{aligned} S &= -0.25 \pm 0.19 \\ T &= -0.12 \pm 0.21 \end{aligned} \tag{3}$$

(with a relative correlation of 0.86) even when  $\delta g_{L,R}^b$  are free to float in the fit. Since  $T$  often gets contributions similar in size to  $\delta g_L^b$ , these bounds can be quite restrictive.

Notice that we need not worry about the possibility of having large cancellations between the new-physics contributions to the oblique parameters and  $\delta g_L^b$  in  $R_b$ . It is true that such a partial cancellation actually happens for  $\Gamma_b$  in the SM, where the loop contributions proportional to  $m_t^2$  in  $T$  and  $\delta g_L^b$  exactly cancel in the limit that  $s_w^2 = \frac{1}{4}$ , and so end up being suppressed by a factor  $s_w^2 - \frac{1}{4}$ . We nevertheless need not consider such a cancellation in  $R_b$  since the oblique parameters (especially  $T$ ) almost completely cancel between  $\Gamma_b$  and  $\Gamma_{\text{had}}$ . Quantitatively, we have [4]:

$$\begin{aligned}\Gamma_b &= \Gamma_b^{SM} \left( 1 - 4.57 \delta g_L^b + 0.828 \delta g_R^b - 0.00452 S + 0.0110 T \right) \\ \Gamma_{\text{had}} &= \Gamma_{\text{had}}^{SM} \left( 1 - 1.01 \delta g_L^b + 0.183 \delta g_R^b - 0.00518 S + 0.0114 T \right) \\ \text{so } R_b &= R_b^{SM} \left( 1 - 3.56 \delta g_L^b + 0.645 \delta g_R^b + 0.00066 S - 0.0004 T \right).\end{aligned}\tag{4}$$

We now turn to a discussion of the circumstances under which the above conditions may be achieved in a broad class of models.

### 3. Tree-Level Effects: Mixing

At tree level the  $Z\bar{b}b$  couplings can be modified if there is mixing amongst the charge  $-\frac{1}{3}$  quarks, or the neutral, colourless vector bosons. Being a tree-level effect it is relatively easy and straightforward to analyze and compare different scenarios. Also, since mixing effects can be large, mixing can provide comparatively large corrections to the  $Z\bar{b}b$ -coupling, such as is needed to modify  $R_b$  through changes to  $g_R^b$ . Not surprisingly, a number of recent models [9][10], [12]-[14] use mixing to try to resolve the  $R_b$  (and  $R_c$ ) discrepancy. Our aim here is to be reasonably general, and so we are content to survey the simplest options, postponing for the moment a more detailed phenomenological analysis.

In general we imagine that all particles having the same spin, colour and electric charge can be related to one another through mass matrices (some of whose entries might be constrained to be zero in particular models due to gauge symmetries or restrictions on the Higgs-field representations). We denote the colour-triplet, charge  $Q = -\frac{1}{3}$ , quarks in the flavour basis by  $B^a$ , and label the corresponding mass eigenstates<sup>5</sup> by  $b^i$ . The

---

<sup>5</sup> We imagine having already diagonalized the SM mass matrices so that in the absence of this non-standard mixing one of the  $B^a$  reduces to the usual  $b$  quark, with a diagonal mass matrix with the  $d$  and  $s$  quarks.



mass-eigenstate quarks,  $b^i$ , are obtained from the  $B^a$  by performing independent unitary rotations,  $\left(\mathcal{U}_{L,R}^\dagger\right)^{ai}$ , amongst the left- and right-handed fields. The  $b$  quark that has been observed in experiments is the lightest of the mass eigenstates,  $b = b^1$ , and all others are necessarily much heavier than this state.

Similar considerations also apply for colourless, electrically-neutral spin-one particles. In this case we imagine the weak eigenstates,  $Z_\mu^w$ , to be related to the mass eigenstates,  $Z_\mu^m$ , by an orthogonal matrix,  $\mathcal{M}^{wm}$ . We take the physical  $Z$ , whose properties are measured in such exquisite detail at LEP and SLC, to be the lightest of the mass eigenstates:  $Z_\mu \equiv Z_\mu^1$ .

Assuming that all of the  $b^i$  and  $Z^m$  (except for the lightest ones, the familiar  $b$  and  $Z$  particles) are too heavy to be directly produced at  $Z$ -resonance energies, we find that the flavour-diagonal effective neutral-current couplings relevant for  $R_b$  are

$$\begin{aligned} g_{L,R}^b &\equiv (g_{m=1})_{L,R}^{11} = \sum_{abw} (g_w)^{ab}_{L,R} \mathcal{U}_{L,R}^{a1*} \mathcal{U}_{L,R}^{b1} \mathcal{M}^{w1} \\ &= \sum_{aw} (g_w^a)_{L,R} \left| \mathcal{U}_{L,R}^{a1} \right|^2 \mathcal{M}^{w1}, \end{aligned} \quad (5)$$

where the neutral-current couplings are taken to be diagonal in the flavour  $B^a$  basis.<sup>6</sup>

This expression becomes reasonably simple in the common situation for which only two particles are involved in the mixing. In this case we may write  $B^a = \begin{pmatrix} B \\ B' \end{pmatrix}$ ,  $b^i = \begin{pmatrix} b \\ b' \end{pmatrix}$  and  $Z^w = \begin{pmatrix} Z \\ Z' \end{pmatrix}$ , and take  $\mathcal{U}_L$ ,  $\mathcal{U}_R$  and  $\mathcal{M}$  to be two-by-two rotation matrices parameterized by the mixing angles  $\theta_L$ ,  $\theta_R$  and  $\theta_Z$ . In this case eq. (5) reduces to

$$g_{L,R}^b = \left[ (g_Z^B)_{L,R} c_{L,R}^2 + (g_Z^{B'})_{L,R} s_{L,R}^2 \right] c_Z + \left[ (g_{Z'}^B)_{L,R} c_{L,R}^2 + (g_{Z'}^{B'})_{L,R} s_{L,R}^2 \right] s_Z, \quad (6)$$

where  $s_L$  denotes  $\sin \theta_L$ , *etc.* Increasing  $R_b$  requires increasing the combination  $(g_L^b)^2 + (g_R^b)^2$ . To see how this works we now specialize to more specific alternatives.

---

<sup>6</sup> Eq. (5) describes the most relevant effects for the  $R_b$  problem, namely the mixing of  $Z$  and  $b$  with new states. However, in general other indirect effects are also present, such as, for example, a shift in  $M_Z$  due to the mixing with the  $Z'$ . For a detailed analysis of the simultaneous effects of mixing with a  $Z'$  and new fermions, see Ref. [15].

### 3.1) $Z$ Mixing

First consider the case where two gauge bosons mix. Then eq. (6) reduces to

$$g_{L,R}^b = (g_Z^B)_{L,R} c_Z + (g_{Z'}^B)_{L,R} s_Z, \quad (7)$$

where  $(g_Z^B)_{L,R}$  is the SM coupling in the absence of  $Z$  mixing, and  $(g_{Z'}^B)_{L,R}$  is the  $b$ -quark coupling to the new field  $Z'_\mu$  (which might itself be generated through  $b$ -quark mixing). It is clear that so long as the  $Z'\bar{b}b$  coupling is nonzero, then it is always possible to choose the angle  $\theta_Z$  to ensure that the total effective coupling is greater than the SM one,  $(g_Z^B)_{L,R}$ . This is because the magnitude of any function of the form  $f(\theta_Z) \equiv A c_Z + B s_Z$  is maximized by the angle  $\tan \theta_Z = B/A$ , for which  $|f|_{\max} = |A/c_Z| \geq |A|$ .

The model-building challenge is to ensure that the same type of modifications do not appear in an unacceptable way in the effective  $Z$  couplings to other fermions, or in too large an  $M_Z$  shift due to the mixing. This can be ensured using appropriate choices for the transformation properties of the fields under the new gauge symmetry, and sufficiently small  $Z$ - $Z'$  mixing angles. Models along these lines have been recently discussed in Refs. [9],[16].

### 3.2) $b$ -Quark Mixing

The second natural choice to consider is pure  $b$ -quark mixing, with no new neutral gauge bosons. We consider only the simple case of  $2 \times 2$  mixings, since with only one new  $B'$  quark mixing with the SM bottom quark, eq. (6) simplifies considerably. As we will discuss below, we believe this to be sufficient to elucidate most of the features of the possible  $b$ -mixing solutions to the  $R_b$  problem.

Let us first establish some notation. We denote the weak  $SU(2)$  representations of the SM  $B_{L,R}$  and of the  $B'_{L,R}$  as  $R_{L,R}$  and  $R'_{L,R}$ , respectively, where  $R = (I, I_3)$ . The SM  $B$ -quark assignments are  $R_L = (\frac{1}{2}, -\frac{1}{2})$  and  $R_R = (0, 0)$ . By definition, a  $B'$  quark must have electric charge  $Q = -1/3$ , but may in principle have arbitrary weak isospin  $R'_{L,R} = (I'_{L,R}, I'_{3L,R})$ .

In terms of the eigenvalues  $I'_{3L}$  and  $I'_{3R}$  of the weak-isospin generator  $I_3$  acting on  $B'_L$  and  $B'_R$ , the combination of couplings which controls  $\Gamma_b$  becomes

$$\Gamma_b \propto (g_L^b)^2 + (g_R^b)^2 = \left( -\frac{c_L^2}{2} + \frac{s_w^2}{3} + s_L^2 I'_{3L} \right)^2 + \left( \frac{s_w^2}{3} + s_R^2 I'_{3R} \right)^2. \quad (8)$$

In order to increase  $\Gamma_b$  using this expression,  $\theta_L$  and  $\theta_R$  must be such as to make  $g_L^b$  more negative,  $g_R^b$  more positive, or both. Two ways to ensure this are to choose

$$I'_{3L} < -\frac{1}{2} \quad \text{or} \quad I'_{3R} > 0. \quad (9)$$

There are also two other alternatives, involving large mixing angles or large  $B'$  representations:  $I'_{3L} > 0$ , with  $s_L^2(I'_{3L} + \frac{1}{2}) > 1 - 2s_w^2/3 \simeq 0.85$ , and  $I'_{3R} < 0$ , with  $s_R^2|I'_{3R}| > 2s_w^2/3 \simeq 0.15$ . Note, however, that charged-current data puts constraints on the LH mixing. This is because, in the presence of such mixing, the CKM elements  $V_{qb}$  ( $q = u, c, t$ ) get rescaled as  $V_{qb} \rightarrow c_L V_{qb}$ , thus leading to a decrease in rates for processes where the  $b$  quark couples to a  $W$ . For example, studies of  $t$ -quark decay at the Tevatron give  $|V_{tb}| = 0.97 \pm 0.15 \pm 0.07$  [17], assuming the validity of the SM. Allowing for  $b$ - $b'$  mixing, this yields a  $2\sigma$  lower limit of  $c_L > 0.64$ . Hence, solutions with large  $s_L$  would require  $I'_{3L} \geq +3/2$  since  $s_L$  is bounded from above. As we will argue, large mixings with  $B'$  of such high values of isospin are theoretically disfavored. In contrast, as discussed below, there are no corresponding limits on the RH mixings, and large  $s_R$  solutions are always acceptable.

We proceed now to classify the models in which the SM bottom quark mixes with other new  $Q = -1/3$  fermions. Although there are endless possibilities for the kind of exotic quark one could consider, the number of possibilities can be drastically reduced, and a complete classification becomes possible, after the following two assumptions are made:

- (i): There are no new Higgs-boson representations beyond doublets and singlets.
- (ii): The usual  $B$ -quark mixes with a single  $B'$ , producing the mass eigenstates  $b$  and  $b'$ . This constrains the mass matrix to be  $2 \times 2$ :

$$(\bar{B} \quad \bar{B}')_L \begin{pmatrix} M_{11} & M_{12} \\ M_{21} & M_{22} \end{pmatrix} \begin{pmatrix} B \\ B' \end{pmatrix}_R. \quad (10)$$

We will examine all of the alternatives consistent with these assumptions, both of which we believe to be well-motivated, and indeed not very restrictive. The resulting models include the “standard” exotic fermion scenarios [18] (vector singlets, vector doublets, mirror fermions), as well as a number of others.

Let us first discuss assumption (i). From Table 1 and eq. (8) one sees that the mixing angles must be at least as large as 10% to explain  $R_b$ , implying that the off-diagonal entries in the mass matrix (10) which give rise to the mixing are of order  $s_{L,R} M_{22} \gtrsim 0.1$  GeV.

If these entries are generated by Higgs fields in higher than doublet representations, even such a small VEV would badly undermine the agreement between theory and experiment for the  $M_W/M_Z$  mass ratio.<sup>7</sup>

Combining assumption (i) with two necessary attributes of the  $B$ – $B'$  mass matrix, it is possible to specify which representations  $R'_{L,R}$  allow the  $B'$  to mix with the  $B$  quark of the SM:

- (1): Since the  $B'$  should be relatively heavy, we require that  $M_{22} \neq 0$ . Then the restriction (i) on the possible Higgs representations implies that

$$|I'_L - I'_R| = 0, \frac{1}{2}; \quad (11)$$

and

$$|I'_{3L} - I'_{3R}| = 0, \frac{1}{2}. \quad (12)$$

- (2): To have  $b$ – $b'$  mixing, at least one of the off-diagonal entries,  $M_{12}$  or  $M_{21}$ , must be nonzero. These terms arise respectively from the gauge-invariant products  $R_M \otimes R_L \otimes \bar{R}'_R$  and  $R_M \otimes R_R \otimes \bar{R}'_L$  or  $R_L \otimes \bar{R}'_R$  and  $R_R \otimes \bar{R}'_L$  so that  $\bar{R}'_{L(R)}$  must transform as the conjugate of the tensor product  $R_M \otimes R_{R(L)}$ :

$$R'_L = R_M \otimes R_R = (0, 0), \left(\frac{1}{2}, \pm\frac{1}{2}\right), \quad (13)$$

or

$$R'_R = R_M \otimes R_L = (0, 0), \left(\frac{1}{2}, -\frac{1}{2}\right), (1, -1), (1, 0). \quad (14)$$

Thus the only possible representations for the  $B'$  are those with  $I'_R = 0, \frac{1}{2}, 1$  and  $I'_L = 0, \frac{1}{2}, 1, \frac{3}{2}$ , subject to the restrictions (11)–(14).

As for assumption (ii), it is of course possible that several species of  $B'$  quarks mix with the  $B$ , rise to an  $N \times N$  mass matrix, but it seems reasonable to study the allowed

---

<sup>7</sup> The contribution of these relatively large non-standard VEVs cannot be effectively compensated by loop-effects. On the other hand, beyond Higgs doublets, the next case of a Higgs multiplet preserving the tree level ratio is that of  $I_{3H} = 3, Y_H = 2$ . Alternative scenarios invoking for example triplets suffer from severe fine-tuning problems. We do not consider such possibilities, which would also require the mixed  $B'$  to belong to similarly high-dimensional representations.

types of mixing one at a time. After doing so it is easy to extend the analysis to the combined effects of simultaneous mixing with multiple  $B'$  quarks. Thus (ii) appears to be a rather mild assumption.

There is one sense in which (ii) might appear to restrict the class of phenomena we look at in a qualitative way: it is possible to obtain mixing between the  $B$  and a  $B'$  in one of the higher representations we have excluded by “bootstrapping,” that is, by intermediate mixing with a  $B'$  in one of those allowed representations. For example, if  $B$  mixes with  $B'_1$  of isospin  $I'_L = \frac{3}{2}$  and the latter mixes with  $B'_2$  of isospin  $I'_L = \frac{5}{2}$ , this would induce mixing between  $B$  and  $B'_2$ . But since mass entries directly coupling  $B$  to  $B'_2$  are forbidden by assumption (i), the  $B$ – $B'_2$  mixing will be proportional to the  $B$ – $B'_1$  mixing, implying that these additional effects are subleading, that is, of higher order in the mixing angles. This means that if the dominant  $B$ – $B'$  mixing effects are insufficient to account for the measured  $R_b$ , adding more  $B'$  with larger isospin cannot improve the situation. So we do not expect assumption (ii) to limit the generality of our conclusions.

We can now enumerate all the possibilities allowed by assumptions (i) and (ii). With the permitted values of  $I'_R$  and  $I'_L$  listed above, and the requirement that at least one of the two conditions (13)–(14) is satisfied, there are 19 possibilities, listed in Table 2. Although not all of them are anomaly-free, the anomalies can always be canceled by adding other exotic fermions which have no effect on  $R_b$ . Since only the values of  $I'_{3L}$  and  $I'_{3R}$  are important for the  $b$  neutral current couplings, for our purpose models with the same  $I'_{3L,R}$  assignments are equivalent, regardless of  $I'_{L,R}$  or differences in the mass matrix or mixing pattern. Altogether there are 12 inequivalent possibilities. Equivalent models are indicated by a prime (') in the ‘Model’ column in Table 2.

Due to gauge invariance and the restriction (i) on the Higgs sector, in several cases one of the off-diagonal entries  $M_{12}$  or  $M_{21}$  in eq. (10) vanishes, leading to a hierarchy between the LH and the RH mixing angles. If the  $b'$  is much heavier than the  $b$ ,  $M_{12} = 0$  yields  $s_L \sim M_{21}/M_{22}$ , while the RH mixing is suppressed by  $M_{22}^{-2}$ . If on the other hand  $M_{21} = 0$ , then the suppression for  $s_L$  is quadratic, leaving  $s_R$  as the dominant mixing angle. For these cases, the subdominant mixings are shown in parentheses in the ‘Mixing’ column in Table 2. Notice that while models 2 and 6 allow for a large right-handed mixing angle solution of the  $R_b$  anomaly, the “equivalent” models 2' and 6' do not, precisely because of such a suppression.

Six choices satisfy one of the two conditions in eq. (9), and hence can solve the  $R_b$  problem using small mixing angles. They are labeled by an asterisk (\*) in Table 2. Three of these models (10–12) satisfy the first condition for solutions using small LH mixings. Since for all these cases  $I'_{3R} < 0$ , a large RH mixing could alternatively yield a solution but

$I'_L$	$I'_{3L}$	$I'_R$	$I'_{3R}$	Model		Mixing
0	0	0	0	1	Vector Singlet	$L$
		1/2	-1/2	$2^{(**)}$	Mirror Family	$L, R$
			+1/2	$3^{(*)}$		$(L), R$
1/2	-1/2	0	0	4	$4^{th}$ Family	—
		1/2	-1/2	$5^{(**)}$	Vector Doublet (I)	$R$
		1	-1	$6^{(**)}$		$R$
			0	$4'$		—
	+1/2	0	0	$\gamma$		$L$
		1/2	+1/2	$8^{(*)}$	Vector Doublet (II)	$(L), R$
		1	0	$\gamma'$		$L$
			+1	$9^{(*)}$		$(L), R$
1	-1	1	-1	$10^{(*)}$	Vector Triplet (I)	$L, (R)$
		1/2	-1/2	$11^{(*)}$		$L, (R)$
	0	1	0	$1'$	Vector Triplet (II)	$L$
		1/2	-1/2	$2'$		$L, (R)$
3/2	-3/2	1	-1	$12^{(*)}$		$L, (R)$
	-1/2	1	-1	$6'$		$(R)$
			0	$4''$		—
	+1/2	1	0	$\gamma''$		$L$

**Table 2**

### Models and Charge Assignments

All the possible models for  $B$ - $B'$  mixing allowed by the assumptions that (i) here are no new Higgs representations beyond singlets and doublets, and (ii) only mixing with a single  $B'$  is considered. The presence of LH or RH mixings which can affect the  $b$  neutral current couplings is indicated under ‘Mixing’. Subleading mixings, quadratically suppressed, are given in parenthesis. Equivalent models, for the purposes of  $R_b$ , are indicated by a prime (') in the ‘Model’ column, while models satisfying eq. (9) and which can account for the deviations in  $R_b$  with small mixing angles, are labeled by an asterisk (\*). Large RH mixing solutions are labeled by a double asterisk (\*\*).

because  $s_R$  is always suppressed with respect to  $s_L$ , this latter possibility is theoretically disfavored. The other three choices (models 3, 8, 9) satisfy the second condition for solutions using small RH mixing. It is noteworthy that in all six models the relevant mixing needed to explain  $R_b$  is automatically the dominant one, while the other, which would exacerbate the problem, is quadratically suppressed and hence negligible in the large  $m_{b'}$  limit. Finally, there are three choices (models 2, 5, 6) which satisfy the second condition for solutions using RH mixing, or (model 2) having  $s_R$  unsuppressed with respect to  $s_L$ . For these  $I'_{3R} < 0$  and there is only RH mixing. They allow for solutions with large RH mixings and are labeled by a double asterisk (\*\*). According to the assumptions made which restrict the allowed  $R'_L$  representations, there are no possibilities with  $I'_{3L}$  large enough to allow for large LH mixing solutions.

In the light of Table 2 we now discuss in more detail the most popular models, as well as some other more exotic possibilities.

- *Vector singlet:* Vector fermions by definition have identical left- and right-handed gauge quantum numbers. A vector singlet (model 1) is one for which  $I'_L = I'_R = 0$ . Inspection of eq. (8) shows that mixing with such a vector-singlet quark always acts to reduce  $R_b$ .<sup>8</sup>

- *Mirror family:* A mirror family (model 2) is a fourth family but with the chiralities of the representations interchanged. Because  $I'_{3L}$  vanishes, LH mixing acts to reduce the magnitude of  $g_L^b$ , and so tends to make the prediction for  $R_b$  worse than in the SM. For sufficiently large RH mixing angles, however, this tendency may be reversed. As was discussed immediately below eq. (9), since  $I'_{3R}$  is negative a comparatively large mixing angle of  $s_R^2 \gtrsim 1/3$  is needed to sufficiently increase  $R_b$ . Such a large RH mixing angle is phenomenologically permitted by all off-resonance determinations of  $g_R^b$  [19]. In fact, the  $b$ -quark production cross section and asymmetry, as measured in the  $\gamma$ - $Z$  interference region [21][22], cannot distinguish between the two values  $s_R^2 = 0$  and  $4s_w/3$ , which yield exactly the same rates.<sup>9</sup> Hence this kind of model can solve the  $R_b$  problem, though perhaps not in the most aesthetically pleasing way. As is shown in Fig. 2, the allowed range of mixing angles is limited to a narrow strip in the  $s_L^2 - s_R^2$  plane.

- *Fourth family:* A fourth family (model 4) cannot resolve  $R_b$  via tree-level effects because the new  $B'$  quark has the same isospin assignments as the SM  $b$  quark, and so they do not

---

<sup>8</sup> A  $Q=+2/3$  vector singlet can however be used to reduce  $R_c$  [10][12][14], provided that steps are taken, as suggested in Section 2 above, to avoid the resulting preference for an unacceptably large value for  $\alpha_s(M_Z)$ .

<sup>9</sup> The current 90% c.l. upper bound  $s_R^2 < 0.010$  [20] holds in the small mixing angle region  $s_R^2 \ll 1/3$ .

mix in the neutral current.<sup>10</sup> Two other possibilities (models  $4'$  and  $4''$ ) yield the same  $I'_{3LR}$  assignments as the fourth family model, and are similarly unsuccessful in explaining  $R_b$  since they do not modify the  $b$  quark neutral current couplings.

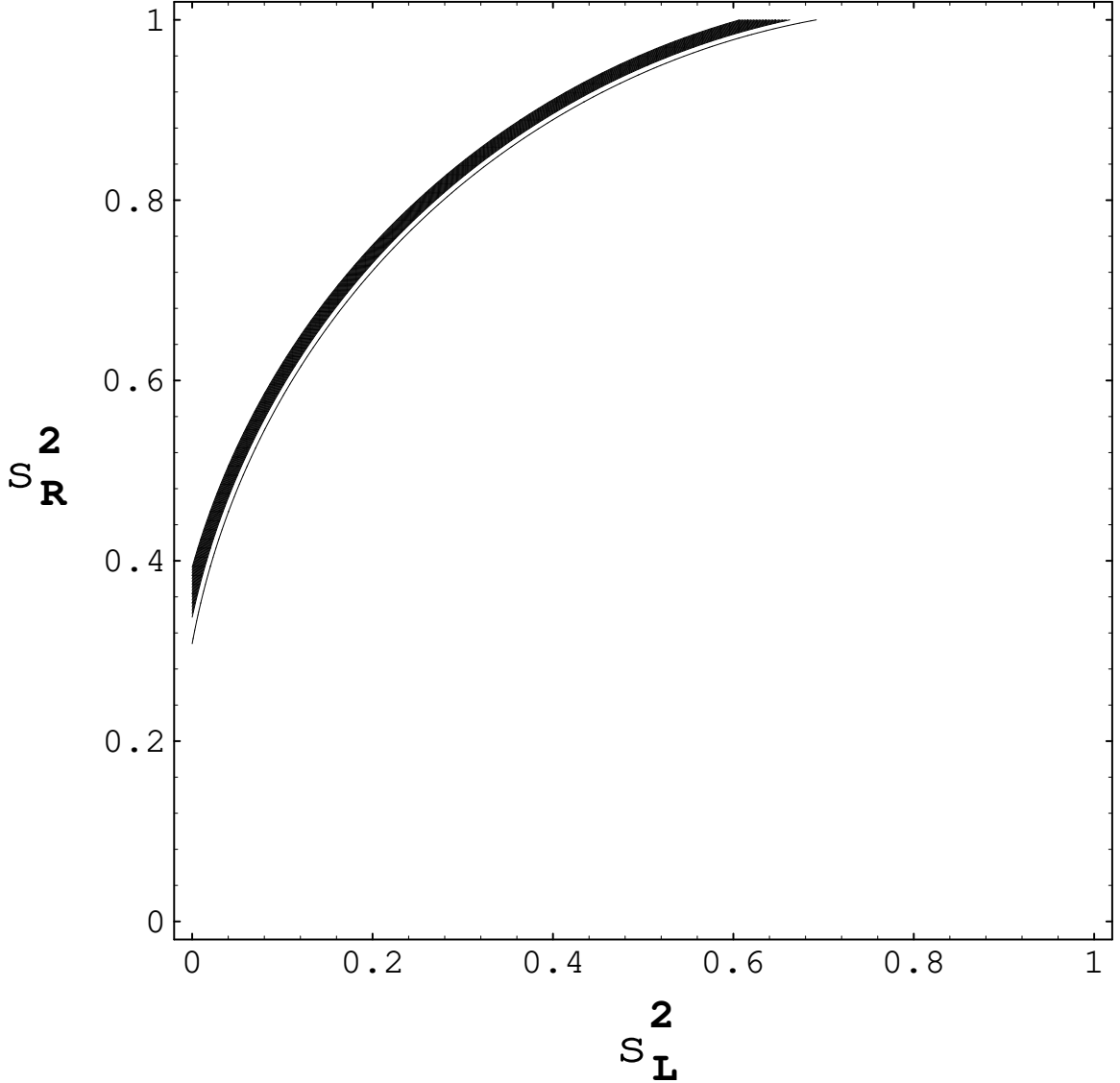


Fig-

ure 2: The experimentally allowed mixing angles for a mirror family. The thick line covers the entire area of values for  $s_L$  and  $s_R$  which are needed to agree with the experimental value for  $R_b$  to the  $2\sigma$  level or better. The thin line represents the one-parameter family of mixing angles which reproduce the SM prediction. Notice that the small-mixing solution, which passes through  $s_L = s_R = 0$ , is ruled out since  $I'_L = 0$  implies that any LH mixing will *reduce*  $g_L^b$  and thus increases the discrepancy with experiment.

---

<sup>10</sup> These models have the further difficulty that, except in certain corners of parameter space [23], they produce too large a contribution to the oblique parameters,  $S$  and  $T$ , to be consistent with the data.



- *Vector doublets*: There are two possibilities which permit a  $Q = -\frac{1}{3}$  quark to transform as a weak isodoublet, and in both cases mixing with the SM  $b$  is allowed. They can be labeled by the different hypercharge value using the usual convention  $Q = I_3 + Y$ .

With the straightforward choice  $I'_{3L} = I'_{3R} = -1/2$  (model 5), we have  $Y'_L = Y'_R = 1/6$ . This type of model is discussed in Ref. [13], where the isopartner of the  $B'$  is a top-like quark  $T'$  having charge  $+\frac{2}{3}$ . Since these are the same charge assignments as for the standard LH  $b$ -quark, this leads to no mixing in the neutral current amongst the LH fields, and therefore only the right-handed mixing angle  $s_R$  is relevant for  $R_b$ . Since  $I'_{3R}$  is negative a comparatively large mixing angle of  $s_R^2 \gtrsim 1/3$  is needed to sufficiently increase  $R_b$ , in much the same way as we found for the mirror-family scenario discussed above. The required mixing angle that gives the experimental value,  $R_b = 0.2219 \pm 0.0017$ , is

$$s_R^2 = 0.367^{+0.013}_{-0.014}. \quad (15)$$

The other way to fit a  $Q = -1/3$  quark into a vector doublet corresponds to  $I'_{3L} = I'_{3R} = +1/2$  (model 8) and so  $Y' = -5/6$  [10]. The partner of the  $B'$  in the doublet is then an exotic quark,  $R$ , having  $Q = -4/3$ . Here  $I'_{3L}$  has the wrong sign for satisfying eq. (9) and so mixing *decreases* the magnitude of  $g_L^b$ . On the other hand,  $I'_{3R}$  has the right sign to increase  $g_R^b$ . Whether this type of model can work therefore depends on which of the two competing effects in  $R_b$  wins. It is easy to see that in this model the  $M_{21}$  entry in the  $B$ - $B'$  mass matrix eq. (10) vanishes, which as discussed above results in a suppression of  $s_L$  quadratic in the large mass, but only a linear suppression for  $s_R$ . Hence,  $s_L$  becomes negligible in the large  $m_{b'}$  limit, leaving  $s_R$  as the dominant mixing angle in  $R_b$ . The mixing angle which reproduces the experimental value for  $R_b$  then is

$$s_R^2 = 0.059^{+0.013}_{-0.015}. \quad (16)$$

However, in order to account for such a large value of the mixing angle in a natural way, the  $b'$  cannot be much heavier than  $\sim 100$  GeV.

Similarly to the  $Y' = -5/6$  vector doublet case, models 3 and 9 also provide a solution through RH mixings. In model 3, the subdominant competing effect of  $s_L$  is further suppressed by a smaller  $I'_{3L}$ , while in model 9 the effect of  $s_R$  is enhanced by  $I'_{3R} = +1$ , and hence a mixing angle a factor of 4 smaller than in (16) is sufficient to explain  $R_b$ .

- *Vector triplets*: There are three possibilities for placing a vector  $B'$  quark in an isotriplet representation:  $I'_{3L} = I'_{3R} = -1, 0, +1$ . The last does not allow for  $b$  mixing, if only Higgs

doublets and singlets are present, and for our purposes,  $I'_{3L} = I'_{3R} = 0$  (model 1') is equivalent to the vector singlet case already discussed. Only the assignment  $I'_{3L} = I'_{3R} = -1$  (model 10) allows for a resolution of the  $R_b$  problem, and it was proposed in Ref. [12]. If  $B'$  is the lowest-isospin member of the triplet there is an exotic quark of charge  $Q = +5/3$  in the model. Again in the limit of large  $b'$  mass one combination of mixing angles (in this case  $s_R$ ) is negligible, due to the vanishing of  $M_{12}$  in eq. (10). As a result,  $s_L$  plays the main role in  $R_b$ . Agreement with experiment requires

$$s_L^2 = 0.0127 \pm 0.0034. \quad (17)$$

Since the resulting change to  $g_L^b$  is so small, such a slight mixing angle would have escaped detection in all other experiments to date.

Similarly to this case, models 11 and 12 also provide a solution through LH mixings. In model 11 the unwanted effects of  $s_R$  are further suppressed, while for model 12 a LH mixing somewhat smaller than in (17) is sufficient to explain the data.

We see from these examples that both  $Z$ -mixing and  $b$ -mixing can in fact resolve the  $R_b$  discrepancy.  $b$ -quark mixing solutions require an exotic new  $B'$  quark with the right electroweak quantum numbers. Solutions with small  $s_R$  and  $s_L$  mixing angles are possible when the  $B'_R$  is the member with highest  $I'_{3R}$  in an isodoublet or isotriplet, or when  $B'_L$  is the member with lowest  $I'_{3L}$  in an isotriplet or isoquartet. In all these cases, new quarks with exotic electric charges are also present. Some other possible solutions correspond to  $I'_{3R} < 0$  and are due to mixing amongst the RH  $b$ -quarks involving fairly large mixing angles. It is intriguing that such large mixing angles are consistent with all other  $b$ -quark phenomenology. In contrast, since the largest value of  $I'_{3L}$  in Table 2 is  $+1/2$ , under our assumptions a large  $s_L$  mixing does not yield any further possibilities.

For some of the models considered, the contributions to the oblique parameters could be problematic, yielding additional constraints. However, for the particular class of vectorlike models (which includes two of the small mixing angle solutions) loop effects are sufficiently small to remain acceptable.<sup>11</sup> This is because, unlike the top quark which belongs to a chiral multiplet, vectorlike heavy  $b'$  quarks tend to decouple in the limit that their masses get large. Introducing mixing with other fermions does produce nonzero oblique corrections, but these remain small enough to have evaded detection. Exceptions to this statement are models involving a large number of new fields, like entire new generations, since these tend to accumulate large contributions to  $S$  and  $T$ .

---

<sup>11</sup> Vectorlike models have the additional advantage of being automatically anomaly free.

## 4. One-Loop Effects: $t$ -Quark Mixing

We now turn to the modifications to the  $Z\bar{b}b$  couplings which can arise at one loop. Recall that this option can only explain  $R_b$  if the LH  $b$ -quark coupling,  $g_L^b$ , receives a negative correction comparable in size to the SM  $m_t$ -dependent contributions. As was argued in section 2, it is the LH coupling we are interested in because a loop-level change in  $g_R^b$  is too small to fix the discrepancy between the SM and experiment.

The fact that the  $R_b$  problem could be explained if the  $m_t$ -dependent one-loop contributions of the SM were absent naturally leads to the idea that perhaps the  $t$ -quark couples differently to the  $b$ -quark than is supposed in the SM. If the  $t$  quark mixed significantly with a new  $t'$  quark one might be able to significantly reduce the relevant contributions below their SM values. In this section we show that it is at best possible to reduce the discrepancy to  $\sim 2\sigma$  in models of this type, and so they cannot claim to completely explain the  $R_b$  data.

Our survey of  $t$ -quark mixing is organized as follows. We first describe the framework of models within which we systematically search, and we identify all of the possible exotic  $t$ -quark quantum numbers which can potentially work. This study is carried out much in the spirit of the analysis of  $b$  mixing presented in section 3. We then describe the possible  $t'$  loop contributions to the neutral-current  $b$  couplings. Since this calculation is very similar to computing the  $m_t$ -dependent effects within the SM, we briefly review the latter. Besides providing a useful check on our final expressions, we find that the SM calculation also has several lessons for the more general  $t$ -quark mixing models.

### 4.1) Enumerating the Models

In this section we identify a broad class of models in which the SM top quark mixes with other exotic top-like fermions. As in the previous section concerning  $b$ -quark mixing, we denote the electroweak eigenstates by capitals,  $T^i$ , and the mass eigenstates by lower-case letters,  $t^a$ . To avoid confusion, quantities which specifically refer to the  $b$  sector will be labeled with the superscript  $B$ . By definition, a  $T'$  quark must have electric charge  $Q = 2/3$ , but may in principle have arbitrary weak isospin  $R'_{L,R} = (I'_{L,R}, I'_{3L,R})$ . Following closely the discussion in the previous section, we make three assumptions which allow for a drastic simplification in the analysis, without much loss of generality:

- (i): First, the usual  $T$ -quark is only allowed to mix with a single  $T'$  quark at a time, producing the mass eigenstates  $t$  and  $t'$ .

- (ii): Second, we assume again that Higgs-bosons appear only in doublet and singlet representations.

- (iii): Finally, certain  $T'$ -quark representations also contain new  $B'$  quarks. We denote the  $B'_L$  and  $B'_R$  as ‘exotic’ whenever they have non-standard weak isospin assignments, that is,  $I'_{3L} \neq -\frac{1}{2}$  or  $I'_{3R} \neq 0$ . As we have already discussed, for exotic  $B'$  quarks  $b$ – $b'$  mixing will modify the  $b$  neutral-current couplings at tree level, overwhelming the loop-suppressed  $t$ – $t'$  mixing effects in  $R_b$ . We therefore carry out our analysis under the requirement that any  $b$ – $b'$  mixing affecting the  $b$  neutral-current couplings be absent.

Our purpose is now to examine all of the alternatives which can arise subject to these three assumptions. According to (i), the  $T$ – $T'$  mass matrices we consider are  $2 \times 2$ , and can be written in the general form

$$(\bar{T} \quad \bar{T}')_L \begin{pmatrix} M_{11} & M_{12} \\ M_{21} & M_{22} \end{pmatrix} \begin{pmatrix} T \\ T' \end{pmatrix}_R. \quad (18)$$

Due to our restriction (ii) on the Higgs sector, certain elements of this mass matrix are nonzero only for particular values of the  $T'$  weak isospin. Moreover, whenever  $T'_R$  belongs to a multiplet which also contains a  $Q = -1/3$   $B'_R$  quark, the  $M_{12}^B$  and  $M_{12}$  entries of the  $B$ – $B'$  and  $T$ – $T'$  mass matrices are the same. In those cases in which the  $B'$  quark is exotic, assumption (iii) then forces us to set  $M_{12} = 0$ . In contrast, the  $M_{21}$  entries are unrelated – for example, the choice  $M_{21}^B = 0$  is always possible even if  $M_{21} \neq 0$  for the  $T$  and  $T'$  quarks.

In order to select those representations,  $R'_{L,R}$ , which can mix with the SM  $T$  quark, we require the following conditions to be satisfied:

- (1): In order to ensure a large mass for the  $t'$ , we require  $M_{22} \neq 0$ . Analogously to (11) and (12), this implies

$$|I'_L - I'_R| = 0, \frac{1}{2}; \quad (19)$$

and

$$|I'_{3L} - I'_{3R}| = 0, \frac{1}{2}. \quad (20)$$

- (2): To ensure a non-vanishing  $t$ – $t'$  mixing we require at least one of the two off-diagonal entries,  $M_{12}$  or  $M_{21}$ , to be non-vanishing. This translates into the following conditions on  $R'_L$  and  $R'_R$ :

$$R'_L = R_M \otimes R_R = (0, 0), \left( \frac{1}{2}, \pm \frac{1}{2} \right), \quad (21)$$

or

$$R'_R = R_M \otimes R_L = (0, 0), \left(\frac{1}{2}, +\frac{1}{2}\right), (1, 0), (1, +1). \quad (22)$$

• (3): Whenever  $R'_R$  contains a  $Q = -1/3$  quark, and either  $B'_L$  or  $B'_R$  have non-standard isospin assignments, we require  $M_{12} = 0$ . This ensures that at tree level the neutral current  $b$  couplings are identical to those of the SM. Clearly, in the cases in which the particular  $R'_L$  representation implies a vanishing  $M_{21}$  element, imposing the condition  $M_{12} = 0$  completely removes all  $t$ - $t'$  mixing.

We now may enumerate all the possibilities. From eqs. (19)–(22), it is apparent that as in the  $B'$  case the only allowed representations must have  $I'_R = 0, \frac{1}{2}, 1$  and  $I'_L = 0, \frac{1}{2}, 1, \frac{3}{2}$ .

Consider first  $I'_L = 1$  or  $\frac{3}{2}$ . In this case, from eq. (21),  $M_{21} = 0$ . Thus, we need  $M_{12} \neq 0$  if there is to be any  $t$ - $t'$  mixing. The four possibilities for  $R'_R$  are shown in eq. (22). Of these,  $R'_R = (0, 0)$  is not allowed since eq. (19) is not satisfied. In addition,  $R'_R = (\frac{1}{2}, \frac{1}{2})$  and  $(1, 0)$  both contain exotic  $B'$  quarks ( $I'_{3R} = -\frac{1}{2}$  or  $-1$ ) and so  $M_{12}$  is forced to vanish, leading to no  $t$ - $t'$  mixing. This leaves  $R'_R = (1, 1)$  as a possibility, since the  $B'_R$  is not exotic ( $I'_{3R} = 0$ ). If we choose  $R'_L$  such that  $I'_{3L} = -\frac{1}{2}$ , then both  $B'_L$  and  $B'_R$  are SM-like, and  $b$ - $b'$  mixing is not prohibited since it does not affect the  $b$  neutral current couplings. Thus, the combination  $R'_L = (\frac{3}{2}, \frac{1}{2})$ ,  $R'_R = (1, 1)$  is allowed.

Next consider  $I'_L = 0$  or  $\frac{1}{2}$ . Here, regardless of the value of  $I'_{3L}$ ,  $M_{21}$  can be nonzero. Thus any  $R'_R$  representation which satisfies eqs. (19) and (20) is permitted. It is straightforward to show that there are 11 possibilities.

The list of the allowed values of  $I'_{3L}$  and  $I'_{3R}$  which under our assumptions lead to  $t$ - $t'$  mixing is shown in Table 3. There are twelve possible combinations, including fourth-generation fermions, vector singlets, vector doublets, and mirror fermions. Not all of these possibilities are anomaly-free, but as already noted one could always cancel anomalies by adding other exotic fermions which give no additional effects in  $R_b$ .

It is useful to group the twelve possibilities into three different classes, according to the particular constraints on the form of the  $T$ - $T'$  mass matrix in eq. (18).

The first two entries in Table 3, which we have assigned to group A, correspond to the special case in which the  $B_{L,R}$  and  $B'_{L,R}$  have the same third component of weak isospin, hence leaving the  $b$  neutral current unaffected by mixing. Because both  $B'_L$  and  $B'_R$  appear in the same multiplets with  $T'_L$  and  $T'_R$ , two elements of the  $B$ -quark and  $T$ -quark mass matrices are equal:

$$M_{12} = M_{12}^B, \quad M_{22} = M_{22}^B. \quad (23)$$

$I'_L$	$I'_{3L}$	$I'_R$	$I'_{3R}$	Model	Group
3/2	+1/2	1	+1		$A_1$
1/2	+1/2	1	+1		$A_2$
			0		$B_1$
		1/2	+1/2	Vector Doublet (I)	$B_2$
		0	0	$4^{th}$ Family	$C_1$
1/2	-1/2	1	0		$B_3$
			-1		$B_4$
		1/2	-1/2	Vector Doublet (III)	$B_5$
		0	0		$C_2$
0	0	1/2	+1/2	Mirror Fermions	$B_6$
			-1/2		$B_7$
		0	0	Vector Singlet	$C_3$

**Table 3**

### Models and Charge Assignments

Values of the weak isospin of  $T'_L$  and  $T'_R$  which, under the only restrictions of singlet and doublet Higgs representations, lead to nonzero  $t$ - $t'$  neutral current mixing. The ‘Model’ column, labels the more familiar possibilities for the  $T'$  quarks: Vector Singlets, Mirror Fermions, Fourth Family and Vector Doublets. The other models are more exotic.

As we will see, this condition is important since it implies a relation between the mixings and the  $m_t, m_{t'}$  mass eigenvalues. Although outside the subject of the present paper, it is noteworthy that for these models the simultaneous presence of both  $b$ - $b'$  and  $t$ - $t'$  mixing generates new, interesting effects in the charged currents: for example, right-handed  $W\bar{t}b$  charged currents get induced, proportional to the product of the mixings of the RH  $T$  and  $B$  quarks.

For the models in group  $B$ , the condition

$$M_{12} = 0 \tag{24}$$

holds. In the four cases corresponding to  $R'_R = (1, 0)$  (models  $B_1, B_3$ ) and  $R'_R = (1/2, 1/2)$  (models  $B_2, B_6$ ), an exotic  $B'_R$  quark is present in the same  $T'_R$  multiplet. Hence  $M_{12}$  has to be set to zero in order to forbid the unwanted tree-level  $b$  mixing effects. In the other

three cases belonging to group  $B$ ,  $T'_R$  corresponds to the lowest component of non-trivial multiplets:  $R'_R = (1, -1)$  (model  $B_4$ ) and  $R'_R = (1/2, -1/2)$  (models  $B_5, B_7$ ). For these values of  $I'_{3R}$ ,  $M_{12} = 0$  is automatically ensured, due to our restriction to Higgs singlets or doublets. Furthermore, these representations do not contain a  $B'_R$  quark, and no  $B'_L$  quark appears in the corresponding  $R'_L$ . There is therefore no  $b$ - $b'$  mixing.

We should also remark that in model  $B_3$  no  $B'_L$ -quark appears in  $R'_L$ . However, a  $B'_L$  is needed as the helicity partner of the  $B'_R$  present in  $R'_R = (1, 0)$ . Because of our restriction on the allowed Higgs representations,  $B'_L$  must belong to  $R'_L = (1, 0)$  or  $R'_L = (1/2, 1/2)$ , which in turn contain a new  $T''_L \neq T'_L$ . While the first choice corresponds to a type of  $T''_L$  mixing which we have already excluded from our analysis, the second choice is allowed and corresponds to model  $B_1$ . Following assumption (i), even in this case we neglect possible  $T''_L$  mixings of type  $B_1$  when analysing  $B_3$ .

Finally, the remaining three models constitute group  $C$ , corresponding to  $R'_R = (0, 0)$ . In this group,  $T'_R$  is an isosinglet, as is the SM  $T_R$ , implying that only LH  $t$ - $t'$  mixing is relevant. For  $C_2$  and  $C_3$ ,  $R'_L$  does not contain a  $B'_L$ , while for  $C_1$  the  $B'_L$  is not exotic. Hence in all the three cases the  $b$  neutral-current couplings are unchanged relative to the SM, and we need not worry about tree-level  $b$ -mixing effects.

#### 4.2) $t$ -Quark Loops Within the Standard Model

Before examining the effect of  $t$ - $t'$  mixing on the radiative correction to  $Z\bar{b}b$ , we first review the SM computation. We follow the notation and calculation of Bernab  , Pich and Santamar  a [11](BPS). The corrections are due to the 10 diagrams of Fig. 3. All diagrams are calculated in 't Hooft-Feynman gauge, and we neglect the  $b$ -quark mass as well as the difference  $|V_{tb}|^2 - 1$ .

Due to the neglect of the  $b$ -quark mass, and due to the LH character of the charged-current couplings, the  $t$ -quark contribution to the  $Z\bar{b}b$  vertex correction preserves helicity. Following BPS we write the helicity-preserving part of the  $Z \rightarrow b\bar{b}$  scattering amplitude as

$$\mathcal{T} = - \left( \frac{e}{s_w c_w} \right) \bar{b}(p_1, \lambda_1) \Gamma^\mu b(p_2, \lambda_2) \epsilon_\mu(q, \lambda), \quad (25)$$

with

$$\Gamma^\mu = \Gamma_0^\mu + \delta \Gamma^\mu, \quad \delta \Gamma^\mu = \frac{\alpha}{2\pi} \gamma^\mu \gamma_L I(s, r). \quad (26)$$

where  $\delta \Gamma^\mu$  represents the loop-induced correction to the  $Z\bar{b}b$  vertex.  $I(s, r)$  is a dimensionless and Lorentz-invariant form factor which depends, *a priori*, on the three independent

ratios:  $r \equiv m_t^2/M_W^2$ ,  $s \equiv M_Z^2/M_W^2$  and  $q^2/M_W^2$ . For applications at the  $Z$  resonance only two of these are independent due to the mass-shell condition  $q^2 = M_Z^2$ . Moreover, for an on-shell  $Z$ , non-resonant box-diagram contributions to  $e^+e^- \rightarrow b\bar{b}$  are unimportant, and  $I(s, r)$  can be treated as an effectively gauge-invariant quantity.

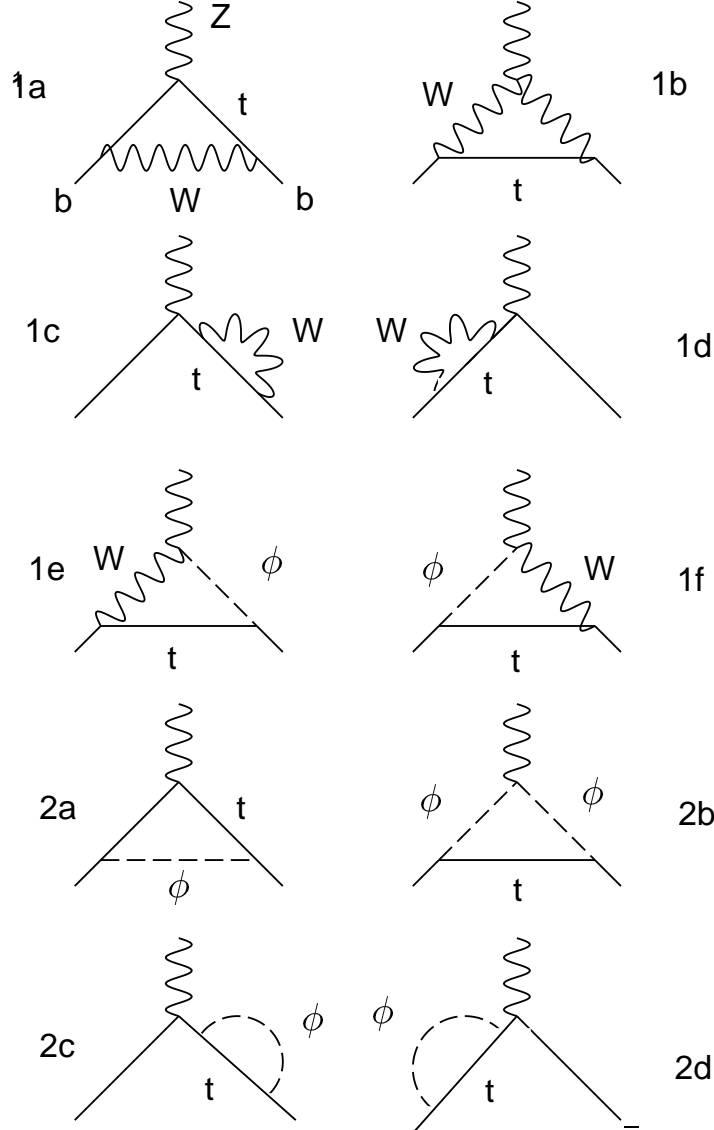


Figure 3: The

Feynman diagrams through which the top quark contributes to the  $Z\bar{b}b$  vertex within the Standard Model.

The contributions due to the  $t$ -quark may be isolated from other radiative corrections by keeping only the  $r$ -dependent part of  $I(s, r)$ . BPS therefore define the difference

$$F(s, r) \equiv I(s, r) - I(s, 0) . \quad (27)$$



Given this function, the  $m_t$ -dependence of the width  $Z \rightarrow b\bar{b}$  is obtained using

$$\Gamma_b^{SM}(r) = \Gamma_b^{SM}(r=0) \left[ 1 + \frac{\alpha}{\pi} \left( \frac{g_L^b}{(g_L^b)^2 + (g_R^b)^2} \right) F^{SM}(s, r) + \text{V.P.}(s, r) \right]. \quad (28)$$

In this last equation  $\text{V.P.}(s, r)$  denotes the  $m_t$ -dependent contributions which enter  $\Gamma_b$  through the loop corrections to the gauge-boson vacuum polarizations.

The function  $F^{SM}(s, r)$  is straightforward to compute. Although the resulting expressions are somewhat obscure, the special case  $s = 0$  reveals some interesting features which are also present in our new-physics calculations, and so we show the  $s = 0$  limit explicitly here. For  $s = 0$ , an evaluation of the graphs of Fig. 3 gives the following expressions:

$$F^{1(a)} = -\frac{1}{2s_w^2} \left\{ \frac{g_L^t}{2} \left[ \frac{r(r-2)}{(r-1)^2} \ln r + \frac{r}{r-1} \right] + g_R^t \left[ \frac{r}{(r-1)^2} \ln r - \frac{r}{r-1} \right] \right\} \quad (29)$$

$$F^{1(b)} = \frac{3c_w^2}{4s_w^2} \left[ \frac{r^2}{(r-1)^2} \ln r - \frac{r}{r-1} \right] \quad (30)$$

$$F^{1(c)+1(d)} = \frac{1}{12} \left[ 1 - \frac{3}{2s_w^2} \right] \left\{ \frac{r^2}{(r-1)^2} \ln r - \frac{r}{r-1} \right\} \quad (31)$$

$$F^{1(e)+1(f)} = \frac{r}{2} \left[ \frac{r}{(r-1)^2} \ln r - \frac{1}{r-1} \right] \quad (32)$$

$$F^{2(a)} = -\frac{r}{4s_w^2} \left\{ \frac{g_R^t}{2} \left[ \Delta + \frac{r(r-2)}{(r-1)^2} \ln r + \frac{2r-1}{r-1} \right] + g_L^t \left[ \frac{r}{(r-1)^2} \ln r - \frac{r}{r-1} \right] \right\} \quad (33)$$

$$F^{2(b)} = -\frac{1}{8} \left[ 1 - \frac{1}{2s_w^2} \right] r \left[ \Delta + \frac{r^2}{(r-1)^2} \ln r - \frac{1}{r-1} \right] \quad (34)$$

$$F^{2(c)+2(d)} = \frac{1}{24} \left[ 1 - \frac{3}{2s_w^2} \right] r \left[ \Delta + \frac{r^2}{(r-1)^2} \ln r - \frac{1}{r-1} \right], \quad (35)$$

with

$$\Delta \equiv \frac{2}{n-4} + \gamma + \ln(M_W^2/4\pi\mu^2) - \frac{3}{2}, \quad (36)$$

where  $n$  is the spacetime dimension arising in dimensional regularization, and

$$g_L^t = \frac{1}{2} - \frac{2}{3}s_w^2, \quad g_R^t = -\frac{2}{3}s_w^2. \quad (37)$$

The picture becomes much simpler after summing the diagrams to obtain the total SM contribution:

$$F^{SM}(s=0, r) = \sum_{i=1(a)}^{2(b)} F^i = \frac{1}{8s_w^2} \left[ \frac{r^2}{r-1} - 6 \frac{r}{r-1} + \frac{r(3r+2)}{(r-1)^2} \ln r \right]. \quad (38)$$

There are two points of interest in this sum. First, it is ultraviolet finite since all of the divergences  $\propto 1/(n-4)$  have cancelled. This is required on general grounds since there can be no  $r$ -dependent divergences in  $I^{SM}(s, r)$ , and so these must cancel in  $F^{SM}(s, r)$ . A similar cancellation also occurs when new physics is included, provided that it respects the  $SU_L(2) \times U_Y(1)$  gauge symmetry and that the complete set of new contributions is carefully included.

The second interesting feature of eq. (38) lies in its dependence on the weak mixing angle,  $s_w$ . Each of the contributions listed in eqs. (29) through (35) has the form  $F^i = (x^i + y^i s_w^2)/s_w^2$ ; however all of the terms involving  $y^i$  have cancelled in the sum, eq. (38). This very general result also applies to all of the new-physics models we consider in subsequent sections. As will be proved in Section 5, the cancellation is guaranteed by electromagnetic gauge invariance, because the terms subleading in  $s_w^2$  are proportional to the *electromagnetic*  $b$ -quark vertex at  $q^2 = 0$ , which must vanish. This gives a powerful check on all of our calculations.

Rather than using complete expressions for  $F(s, r)$ , we find it more instructive to quote our results in the limit  $r \gg 1$ , where powers of  $1/r$  and  $s/r$  may be neglected. We do the same for the ratio of masses of other new particles to  $M_W^2$  when these arise in later sections. Besides permitting compact formulae, this approximation also gives numerically accurate expressions for most of the models' parameter range, as is already true for the SM, even though  $r$  in this case is only  $\sim 4$ . In the large- $r$  limit  $F^{SM}(s, r)$  becomes

$$F^{SM}(r) \rightarrow \frac{1}{8s_w^2} \left[ r + \left( 3 - \frac{s}{6}(1 - 2s_w^2) \right) \ln r \right] + \dots, \quad (39)$$

where the ellipsis denotes terms which are finite as  $r \rightarrow \infty$ . Several points are noteworthy in this expression.

- 1: The  $s$ -dependent term appearing in eq. (39) is numerically very small, changing the coefficient of  $\ln r$  from 3 to 2.88. This type of  $s$ -dependence is of even less interest when we consider new physics, since our goal is then to examine whether the new physics can explain the discrepancy between theory and experiment in  $R_b$ . That is, we want to see if the radiative corrections can have the right sign and magnitude to change  $\Gamma_b$  by the correct amount. For these purposes, so long as the inclusion of  $q^2$ -dependent terms only changes the numerical analysis by factors  $\lesssim 25\%$  (as opposed to changing its overall sign) they may be neglected.
- 2: The above-mentioned cancellation of the terms proportional to  $s_w^2$  when  $s = 0$  no longer occurs once the  $s$ -dependence is included. This is as expected since the electromagnetic Ward identity only enforces the cancellation at  $q^2 = 0$ , corresponding to  $s = 0$  in

the present case. Notice that the leading term, proportional to  $r$ , is  $s$ -independent, and because of the cancellation it is completely attributable to graph (2a) of Fig. 3. All of the other graphs cancel in the leading term. Due to its intrinsic relation with the cancellation of the  $s_w^2$ -dependent terms, the fact that only one graph is responsible for the leading contribution to  $\delta g_L^b$  still holds once new physics is included. This will prove useful for identifying which features of a given model control the overall sign of the new contribution to  $\delta g_L^b$ .

- 3: Since the large- $r$  limit corresponds to particle masses (in this case  $m_t$ ) that are large compared to  $M_w$  and  $M_Z$ , this is the limit where the effective-lagrangian analysis described in Section 2 directly applies. Then the function  $F$  can be interpreted as the effective  $Z\bar{b}b$  coupling generated when the heavy particle is integrated out. Quantitatively,  $\delta g_L^b$  is related to  $F$  by

$$\delta g_L^b = \left(\frac{\alpha}{2\pi}\right) F. \quad (40)$$

- 4: The vacuum polarization contributions to  $\Gamma_b$  of eq. (28) have a similar interpretation in the heavy-particle limit. In this case the removal of the heavy particles can generate oblique parameters, which also contribute to  $\Gamma_b$ . In the heavy-particle limit eq. (28) therefore reduces to the first of eqs. (4).

#### 4.3) $\delta g_L^b$ in the $t$ -Quark Mixing Models

We may now compute how mixing in the top-quark sector can affect the loop contributions to the process  $Z \rightarrow b\bar{b}$ . As in the SM analysis, we set  $m_b = 0$ . In addition, following the discussion in the previous subsection, we neglect the  $s$ -dependence in all our expressions. We also ignore all vacuum-polarization effects, knowing that they essentially cancel in  $R_b$ . Finally, in the CKM matrix, we set  $|V_{id}| = |V_{is}| = 0$  where  $i = t, t'$ . Thus, the charged-current couplings of interest to us are described by a  $2 \times 2$  mixing matrix, just as in the neutral-current sector. In the absence of  $t$ - $t'$  mixing this condition implies  $|V_{tb}| = 1$ . our results).

For  $t$ - $t'$  mixing, independent of the weak isospin of the  $T'$ , we write

$$\begin{pmatrix} T \\ T' \end{pmatrix}_{L,R} = \mathcal{U}_{L,R} \begin{pmatrix} t \\ t' \end{pmatrix}_{L,R}, \quad \mathcal{U}_L = \begin{pmatrix} c_L & s_L \\ -s_L & c_L \end{pmatrix}, \quad \mathcal{U}_R = \begin{pmatrix} c_R & -s_R \\ s_R & c_R \end{pmatrix}. \quad (41)$$

where  $c_L \equiv \cos \theta_L$ , etc.. The matrices  $\mathcal{U}_{L,R}$  are analogous to the  $b$ - $b'$  mixing matrices defined in eq. (5) in our tree-level analysis of  $b$  mixing. In order to avoid confusion, in the

present section we define the mixing angles and mass-matrix entries for the  $b$ -quark sector with a superscript  $B$ .

In the presence of  $t$ – $t'$  mixing, the diagonal neutral-current couplings are modified:

$$g_{L,R}^i = \sum_{a=T,T'} g_{L,R}^a (\mathcal{U}_{L,R}^{ai})^2 \equiv g_{L,R}^{t,SM} + \tilde{g}_{L,R}^i, \quad (42)$$

where  $i = t, t'$ , and  $g_{L,R}^{t,SM}$  are the SM couplings defined in eq. (37). The new terms  $\tilde{g}_{L,R}^i$  explicitly read

$$\tilde{g}_L^t = \left( I'_{3L} - \frac{1}{2} \right) s_L^2, \quad \tilde{g}_R^t = I'_{3R} s_R^2, \quad (43)$$

$$\tilde{g}_L^{t'} = \left( I'_{3L} - \frac{1}{2} \right) c_L^2, \quad \tilde{g}_R^{t'} = I'_{3R} c_R^2. \quad (44)$$

In addition, flavour-changing neutral-current (FCNC) couplings will be induced if the  $T'_{L,R}$  has nonstandard isospin assignments,  $I'_{3L} \neq 1/2$  or  $I'_{3R} \neq 0$ :

$$g_{L,R}^{ij} = \sum_{a=T,T'} g_{L,R}^a \mathcal{U}_{L,R}^{ai} \mathcal{U}_{L,R}^{aj} \equiv \tilde{g}_{L,R}^{ij}, \quad (45)$$

where  $i, j = t, t'$ , and  $i \neq j$ . Here,

$$\tilde{g}_L^{tt'} = \left( \frac{1}{2} - I'_{3L} \right) s_L c_L, \quad \tilde{g}_R^{tt'} = I'_{3R} s_R c_R. \quad (46)$$

Eq. (41) determines the effective  $t$  and  $t'$  neutral-current couplings (eqs. (42)–(46)). However, the charged-current couplings depend on the matrix  $\mathcal{V} = \mathcal{U}_L^\dagger \mathcal{U}_L^B$ . Hence we need to also consider  $b$  mixing, since, as discussed in Sec. 4.1, in those cases in which the  $B'$  quark is not exotic ( $I'_{3L} = -1/2$ ,  $I'_{3R} = 0$ ), we have no reason to require  $\mathcal{U}_L^B = I$  (*i.e.* no  $b$ – $b'$  mixing). We then define the  $2 \times 2$  charged current mixing matrix

$$\mathcal{V} = \mathcal{U}_L^\dagger \mathcal{U}_L^B; \quad \mathcal{V}_{tb} \equiv c_L c_L^B + s_L s_L^B, \quad \mathcal{V}_{t'b} \equiv s_L c_L^B - c_L s_L^B, \quad (47)$$

which trivially satisfies the orthogonality conditions  $\mathcal{V} \mathcal{V}^\dagger = \mathcal{V}^\dagger \mathcal{V} = I$ . In the absence of  $b$ – $b'$  mixing, clearly  $\mathcal{V}_{tb} \rightarrow c_L$ ,  $\mathcal{V}_{t'b} \rightarrow s_L$ . We also note that, by assumption, whenever  $\mathcal{V} \neq \mathcal{U}_L$  we necessarily have  $I'_{3L} = +1/2$  (so that  $I'_{3L} = -1/2$ ) in order to guarantee that

the  $B'_L$  is not exotic. From eqs. (43), (44) and (46), this implies that  $\tilde{g}_L^t = \tilde{g}_L^{t'} = \tilde{g}_L^{tt'} = 0$ , that is, the mixing effects on the LH  $t$  and  $t'$  neutral-current couplings vanish.

The Feynman rules of relevance for computing the  $Z\bar{b}b$  vertex loop corrections in the presence of a mixing in the top-quark sector can now be easily written down:

$$\begin{aligned}
W\bar{t}_i b &: \frac{ig}{\sqrt{2}} \mathcal{V}_{t_i b} \gamma_\mu \gamma_L \\
\phi\bar{t}_i b &: \frac{ig}{\sqrt{2}M_W} \mathcal{V}_{t_i b} m_i \gamma_R \\
Z\bar{t}_i t_i &: \frac{ig}{c_w} \gamma_\mu \left[ (g_L^{t,SM} \gamma_L + g_R^{t,SM} \gamma_R) + (\tilde{g}_L^{t_i} \gamma_L + \tilde{g}_R^{t_i} \gamma_R) \right], \\
Z\bar{t} t' &: \frac{ig}{c_w} \gamma_\mu \left[ \tilde{g}_L^{tt'} \gamma_L + \tilde{g}_R^{tt'} \gamma_R \right],
\end{aligned} \tag{48}$$

where  $\phi$  are the unphysical charged scalars, and  $t_i = t, t'$ . The vertices listed in eq. (48) reduce to the SM Feynman rules in the limit of no mixing.

As pointed out at the end of subsection 4.1, in some groups of models equalities can be found between some elements of the  $T$ – $T'$  and  $B$ – $B'$  mass matrices. These have important consequences. In particular, once expressed in terms of the physical masses and mixing angles, the equalities of eq. (23) (which hold in the models of group  $A$ ) can be written

$$[\mathcal{U}_L M_{\text{diag}} \mathcal{U}_R^\dagger]_{a2} = [\mathcal{U}_L^B M_{\text{diag}}^B \mathcal{U}_R^{B\dagger}]_{a2} = (\mathcal{U}_L^B)_{a2} m_B c_R^B; \quad (a = 1, 2), \tag{49}$$

where  $M_{\text{diag}} = \text{diag}[m_t, m_{t'}]$ , and we have used  $M_{\text{diag}}^B = \delta_{i2} m_B$  (recall that we take  $m_b = 0$ ). Multiplying now on the left by  $(\mathcal{U}_L^{B\dagger})_{1a}$  and summing over  $a$  we obtain

$$[\mathcal{V}^\dagger M_{\text{diag}} \mathcal{U}_R^\dagger]_{12} = m_t \mathcal{V}_{tb} s_R + m_{t'} \mathcal{V}_{t'b} c_R = 0. \tag{50}$$

For the models in group  $B$ , the vanishing of  $M_{12}$  implies no  $b$  mixing. Then  $\mathcal{V} = \mathcal{U}_L$ , and eq. (49) still holds in the limit  $\mathcal{V}_{tb} \rightarrow c_L$ ,  $\mathcal{V}_{t'b} \rightarrow s_L$ . For the models in group  $C$  no particular relation between masses and mixing angles can be derived. For example, it is clear that in the 4<sup>th</sup> family model  $C_1$ , eq. (50) does not hold. However, for all these models  $I'_{3R} = 0$ . Hence, noting that all the  $\tilde{g}_R$  couplings in eqs. (43), (44) and (46) are proportional to  $I'_{3R}$ , and defining  $r' = m_{t'}^2/M_W^2$ , squaring eq. (50) yields a relation which holds for all models in Table 3:

$$\mathcal{V}_{tb}^2 \tilde{g}_R^t r = \mathcal{V}_{t'b}^2 \tilde{g}_R^{t'} r' = -\mathcal{V}_{tb} \mathcal{V}_{t'b} \tilde{g}_R^{tt'} \sqrt{rr'}. \tag{51}$$

This relation is used extensively in the calculation which follows.

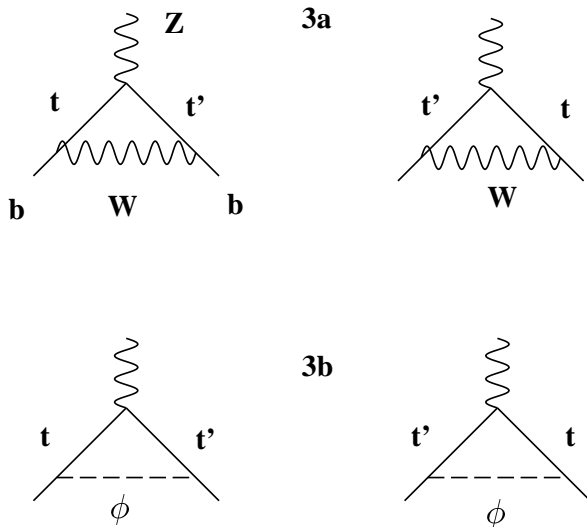


Figure 4: The additional Feynman diagrams which are required for models in which the  $t$  quark mixes with an exotic, heavy  $t'$  quark.

How do we generalize the SM radiative correction to include  $t$ - $t'$  mixing? First note that for each of the diagrams in Fig. 3, there is also a diagram in which all the  $t$ -quarks are replaced by  $t'$ -quarks. Second, there are 2 new diagrams (Fig. 4) due to the FCNC coupling of the  $Z$  to the  $t$  and  $t'$ . So to generalize the SM result to the case of mixing, three things have to be done:

- (i): multiply eqs. (29)-(35) by  $\mathcal{V}_{tb}^2$  for the  $t$  contribution and  $\mathcal{V}_{t'b}^2$  for  $t'$  (with  $r \rightarrow r'$ ),
- (ii): replace  $g_{L,R}^t$  by the modified couplings in eq. (42), adding eqs. (43) and (44) respectively for  $t$  and  $t'$ ,
- (iii): include diagrams 3(a) and 3(b) (Fig. 4) corresponding to the FCNC couplings (eqs. (45)-(46)).

A glance at the Feynman rules in eq. (48) shows that in the first step (i), a correction proportional to  $g_{L,R}^{t,SM}$ , and independent of the  $\tilde{g}_{L,R}$  couplings, is generated. This correction is common to all models in Table 3 – it appears even in the case in which the  $t$  NC couplings are not affected (4<sup>th</sup> family). In contrast, steps (ii) and (iii) generate corrections which differ for different models. It is useful to recast them into two types, one proportional to the LH neutral current couplings ( $\propto \mathcal{V}_{ib} \mathcal{V}_{jb} \tilde{g}_L$ ), and the other proportional to the RH

neutral current couplings ( $\propto \mathcal{V}_{ib} \mathcal{V}_{jb} \tilde{g}_R$ ). The LH and RH corrections vanish respectively for  $I'_{3L} = +1/2$  and  $I'_{3R} = 0$ , when the corresponding neutral-current couplings are not affected by the mixing.

In the presence of mixing, the correction due to the diagrams of Fig. 3 involving internal  $t$ -quarks becomes

$$\sum_{i=1(a)}^{2(b)} F^i = \mathcal{V}_{tb}^2 \left[ F^{SM}(r) + \tilde{F}(\tilde{g}_{L,R}^t, r) \right] , \quad (52)$$

where  $F^{SM}(r)$  is given by eq. (38) and

$$\tilde{F}(\tilde{g}_{L,R}^t, r) = \frac{1}{8s_w^2} \left[ \tilde{g}_L^t r \left( 2 - \frac{4}{r-1} \ln r \right) - \tilde{g}_R^t r \left( \Delta + \frac{2r-5}{r-1} + \frac{r^2-2r+4}{(r-1)^2} \ln r \right) \right] . \quad (53)$$

The third step (iii) gives rise to a new contribution

$$F^{3(a)} + F^{3(b)} = \mathcal{V}_{tb} \mathcal{V}_{t'b} \tilde{F}(\tilde{g}_{L,R}^{tt'}, r, r') . \quad (54)$$

Evaluating diagrams 3(a) and 3(b) (Fig. 4) we find

$$F^{3(a)} = -\frac{1}{s_w^2} \mathcal{V}_{tb} \mathcal{V}_{t'b} \left\{ \frac{1}{2} \tilde{g}_L^{tt'} \frac{1}{r'-r} \left[ \frac{r'^2}{r'-1} \ln r' - \frac{r^2}{r-1} \ln r \right] - \tilde{g}_R^{tt'} \sqrt{rr'} \frac{1}{r'-r} \left[ \frac{r'}{r'-1} \ln r' - \frac{r}{r-1} \ln r \right] \right\} \quad (55)$$

$$F^{3(b)} = \frac{1}{4s_w^2} \mathcal{V}_{tb} \mathcal{V}_{t'b} \left\{ 2 \tilde{g}_L^{tt'} \frac{rr'}{r'-r} \left[ \frac{r'}{r'-1} \ln r' - \frac{r}{r-1} \ln r \right] - \tilde{g}_R^{tt'} \sqrt{rr'} \left( \Delta + 1 + \frac{1}{r'-r} \left[ \frac{r'^2}{r'-1} \ln r' - \frac{r^2}{r-1} \ln r \right] \right) \right\} . \quad (56)$$

Putting all the contributions together, for the general case we find

$$F = \sum_{i=1(a)}^{3(b)} F^i = \sum_{j=1,2} \mathcal{V}_{t_j b}^2 \left[ F^{SM}(r_j) + \tilde{F}(\tilde{g}_{L,R}^{t_j}, r_j) \right] + \mathcal{V}_{tb} \mathcal{V}_{t'b} \tilde{F}(\tilde{g}_{L,R}^{tt'}, r, r') . \quad (57)$$

where  $t_j = t, t'$  and  $r_j = r, r'$ . We note that due to eq. (51) all the divergent terms proportional to  $\tilde{g}_R \Delta$  cancel in the sum. Now, the *correction*  $\delta g_L^b = \frac{\alpha}{2\pi} X_{corr}$  to the SM

result can be explicitly extracted from eq. (57) by means of the relation  $\mathcal{V}_{tb}^2 = 1 - \mathcal{V}_{t'b}^2$ . Moreover, as anticipated it is possible to divide the various contributions to  $X_{corr}$  into three different pieces: a universal correction, a correction due to LH mixing only, and a correction due to the RH mixing. Hence we write

$$X_{corr} \equiv F - F^{SM} = X_{corr}^{Univ} + X_{corr}^{LH} + X_{corr}^{RH} , \quad (58)$$

where

$$X_{corr}^{Univ} = \mathcal{V}_{t'b}^2 [F^{SM}(r') - F^{SM}(r)] , \quad (59)$$

$$X_{corr}^{LH} = \mathcal{V}_{tb}^2 \tilde{F}(\tilde{g}_L^t, r) + \mathcal{V}_{t'b}^2 \tilde{F}(\tilde{g}_L^{t'}, r') + \mathcal{V}_{tb} \mathcal{V}_{t'b} \tilde{F}(\tilde{g}_L^{tt'}, r, r') , \quad (60)$$

$$X_{corr}^{RH} = \mathcal{V}_{tb}^2 \tilde{F}(\tilde{g}_R^t, r) + \mathcal{V}_{t'b}^2 \tilde{F}(\tilde{g}_R^{t'}, r') + \mathcal{V}_{tb} \mathcal{V}_{t'b} \tilde{F}(\tilde{g}_R^{tt'}, r, r') . \quad (61)$$

Using the explicit expressions for  $\tilde{g}_{L,R}^t$ ,  $\tilde{g}_{L,R}^{t'}$  and  $\tilde{g}_{L,R}^{tt'}$  as given in eqs. (43), (44) and (46) above, together with relation (51) for the RH piece, these read

$$X_{corr}^{Univ} = \mathcal{V}_{t'b}^2 f_1^{corr}(r, r') \quad (62)$$

$$X_{corr}^{LH} = (1 - 2I'_{3L}) \mathcal{V}_{tb} \mathcal{V}_{t'b} s_L c_L f_2^{corr}(r, r') \quad (63)$$

$$X_{corr}^{RH} = (2I'_{3R}) \mathcal{V}_{tb}^2 s_R^2 f_3^{corr}(r, r') \quad (64)$$

with

$$f_1^{corr}(r, r') = \frac{1}{8s_w^2} \left\{ \frac{r'(r'-6)}{r'-1} + \frac{r'(3r'+2)}{(r'-1)^2} \ln r' - \frac{r(r-6)}{r-1} - \frac{r(3r+2)}{(r-1)^2} \ln r \right\} , \quad (65)$$

$$f_2^{corr}(r, r') = \frac{1}{8s_w^2} \left\{ \frac{c_L \mathcal{V}_{t'b}}{s_L \mathcal{V}_{tb}} \left( -r' + \frac{2r'}{r'-1} \ln r' \right) + \frac{s_L \mathcal{V}_{tb}}{c_L \mathcal{V}_{t'b}} \left( -r + \frac{2r}{r-1} \ln r \right) \right. \\ \left. + \frac{2r'^2(r-1)}{(r'-1)(r'-r)} \ln r' - \frac{2r^2(r'-1)}{(r-1)(r'-r)} \ln r \right\} , \quad (66)$$

$$f_3^{corr}(r, r') = \frac{1}{8s_w^2} r \left\{ -\frac{1}{2} \left[ \frac{2r-5}{r-1} + \frac{r^2-2r+4}{(r-1)^2} \ln r \right] - \frac{1}{2} \left[ \frac{2r'-5}{r'-1} + \frac{r'^2-2r'+4}{(r'-1)^2} \ln r' \right] \right. \\ \left. - 4 \frac{1}{r'-r} \left[ \frac{r'}{r'-1} \ln r' - \frac{r}{r-1} \ln r \right] + \left[ 1 + \frac{1}{r'-r} \left( \frac{r'^2}{r'-1} \ln r' - \frac{r^2}{r-1} \ln r \right) \right] \right\} . \quad (67)$$



Note that a value of  $V_{tb}$  different from unity can be easily accounted for by using the unitary condition  $|\mathcal{V}_{tb}|^2 + |\mathcal{V}_{t'b}|^2 = |V_{tb}|^2 \equiv 1 - |V_{ts}|^2 + |V_{td}|^2$  in eqs. (62)–(67).

As we have already pointed out, because of our requirement of no  $B$ – $B'$  mixing when the  $B'$  is exotic, only when  $I'_{3L} = +1/2$  can we have  $c_L \neq \mathcal{V}_{tb}$ ,  $s_L \neq \mathcal{V}_{t'b}$ . However, in this case  $X_{corr}^{LH}$  vanishes. Hence, without loss of generality, we can set the LH neutral current mixing equal to the charged current mixing in  $X_{corr}^{LH}$ , obtaining

$$X_{corr}^{LH} = (1 - 2I'_{3L}) \mathcal{V}_{tb}^2 \mathcal{V}_{t'b}^2 f_2^{corr}(r, r'), \quad (68)$$

$$f_2^{corr}(r, r') = \frac{1}{8s_w^2} \left\{ -(r + r') + \frac{2rr'}{r' - r} \ln \frac{r'}{r} \right\}. \quad (69)$$

From eqs. (62), (64) and (68) we see that there are only two independent mixing parameters relevant for the complete analysis of our problem: the LH matrix element  $\mathcal{V}_{tb}$  and the RH mixing  $s_R$ . Furthermore, note that as  $r' \rightarrow r$ , all the corrections in eqs. (65), (67) and (69) vanish, independent of the mixing angles. This comes about because of a GIM-like mechanism for all the pieces which do not depend on  $I'_{3R}$ . The  $I'_{3R}$ -dependent contribution from the RH fermions coupling to the  $Z$  vanishes in the limit  $r' \rightarrow r$  as a consequence of eq. (50).

In the limit  $r, r' \gg 1$ , for the functions  $f_i^{corr}(r, r')$  we obtain

$$f_1^{corr}(r, r') \rightarrow \frac{1}{8s_w^2} \left\{ r' - r + 3 \ln \left( \frac{r'}{r} \right) \right\}, \quad (70)$$

$$f_2^{corr}(r, r') \rightarrow \frac{1}{8s_w^2} \left\{ -(r + r') + \frac{2rr'}{r' - r} \ln \left( \frac{r'}{r} \right) \right\}, \quad (71)$$

$$f_3^{corr}(r, r') \rightarrow \frac{1}{8s_w^2} \left\{ -r + \frac{1}{2} \left( 1 + \frac{r}{r'} \right) \frac{rr'}{r' - r} \ln \left( \frac{r'}{r} \right) - \frac{3r}{r' - r} \ln \left( \frac{r'}{r} \right) + \frac{3}{2} \left( 1 + \frac{r}{r'} \right) \right\}. \quad (72)$$

Let us now consider the numerical values of these corrections in more detail. Using  $m_t = 180$  GeV,  $M_W = 80$  GeV, and  $s_w^2 = 0.23$ , eq. (38) gives a SM radiative correction of

$$F^{SM} = 4.01. \quad (73)$$

The question is whether it is possible to cancel this correction, thus eliminating the  $R_b$  problem, by choosing particular values of  $m_{t'}$  and the mixing angles. For various values of  $m_{t'}$ , the value of  $X_{corr}$  (eq. (58)) is shown in Table 4.

$m_{t'}$	$X_{corr}$
75 GeV	$-3.31 \mathcal{V}_{t'b}^2 - 1.21 (1 - 2I'_{3L}) \mathcal{V}_{t'b}^2 \mathcal{V}_{tb}^2 + 1.39 (2I'_{3R}) \mathcal{V}_{tb}^2 s_R^2$
100 GeV	$-2.70 \mathcal{V}_{t'b}^2 - 0.71 (1 - 2I'_{3L}) \mathcal{V}_{t'b}^2 \mathcal{V}_{tb}^2 + 0.59 (2I'_{3R}) \mathcal{V}_{tb}^2 s_R^2$
125 GeV	$-1.97 \mathcal{V}_{t'b}^2 - 0.34 (1 - 2I'_{3L}) \mathcal{V}_{t'b}^2 \mathcal{V}_{tb}^2 + 0.22 (2I'_{3R}) \mathcal{V}_{tb}^2 s_R^2$
150 GeV	$-1.14 \mathcal{V}_{t'b}^2 - 0.10 (1 - 2I'_{3L}) \mathcal{V}_{t'b}^2 \mathcal{V}_{tb}^2 + 0.05 (2I'_{3R}) \mathcal{V}_{tb}^2 s_R^2$
175 GeV	$-0.20 \mathcal{V}_{t'b}^2 - 0.003 (1 - 2I'_{3L}) \mathcal{V}_{t'b}^2 \mathcal{V}_{tb}^2 + 0.001 (2I'_{3R}) \mathcal{V}_{tb}^2 s_R^2$
200 GeV	$0.84 \mathcal{V}_{t'b}^2 - 0.04 (1 - 2I'_{3L}) \mathcal{V}_{t'b}^2 \mathcal{V}_{tb}^2 + 0.02 (2I'_{3R}) \mathcal{V}_{tb}^2 s_R^2$
225 GeV	$1.97 \mathcal{V}_{t'b}^2 - 0.23 (1 - 2I'_{3L}) \mathcal{V}_{t'b}^2 \mathcal{V}_{tb}^2 + 0.07 (2I'_{3R}) \mathcal{V}_{tb}^2 s_R^2$
250 GeV	$3.20 \mathcal{V}_{t'b}^2 - 0.55 (1 - 2I'_{3L}) \mathcal{V}_{t'b}^2 \mathcal{V}_{tb}^2 + 0.15 (2I'_{3R}) \mathcal{V}_{tb}^2 s_R^2$
275 GeV	$4.52 \mathcal{V}_{t'b}^2 - 1.01 (1 - 2I'_{3L}) \mathcal{V}_{t'b}^2 \mathcal{V}_{tb}^2 + 0.24 (2I'_{3R}) \mathcal{V}_{tb}^2 s_R^2$
300 GeV	$5.93 \mathcal{V}_{t'b}^2 - 1.61 (1 - 2I'_{3L}) \mathcal{V}_{t'b}^2 \mathcal{V}_{tb}^2 + 0.34 (2I'_{3R}) \mathcal{V}_{tb}^2 s_R^2$

**Table 4**

Dependence of the  $t$ - $t'$  Mixing Results on  $m_{t'}$ : This table indicates the dependence on the mass of the  $t'$  quark of the corrections to  $g_L^b$  due to  $t$ - $t'$  mixing, with the  $t$  mass fixed at 180 GeV.

We see that even for  $m_{t'} > m_t$ , it is possible to choose  $I'_{3L}$ ,  $I'_{3R}$ , and the LH and RH mixing angles such that the correction is negative. So the discrepancy in  $R_b$  between theory and experiment can indeed be reduced via  $t$ - $t'$  mixing.

Referring to the models listed in Table 4, the optimal choice for the weak isospin of the  $T'$  is  $I'_{3L} = -1/2$  and  $I'_{3R} = -1$ , regardless of the value of  $m_{t'}$ . Furthermore, maximal RH mixing,  $s_R^2 \sim 1$ , is also preferred. However, even with these choices, it is evidently impossible to completely remove the  $R_b$  problem. From the above table, the best we can do is to take  $m_{t'} = 75$  GeV and  $\mathcal{V}_{t'b}^2 = s_L^2 = 0.6$ , in which case the total correction is  $X_{corr} = -3.68$ . This leaves a  $1.5\sigma$  discrepancy in  $R_b$ , which would put it in the category of the other marginal disagreements between experiment and the SM. However, such a light  $t'$  quark has other phenomenological problems. In particular, CDF has put a lower limit of 91 GeV on charge 2/3 quarks which decay primarily to  $Wb$  [24]. Unless one adds other new physics to evade this constraint, the lightest  $t'$  allowed is about  $m_{t'} \sim 100$  GeV. In this case, maximal LH mixing ( $\mathcal{V}_{t'b}^2 = s_L^2 \sim 1$ ) gives the largest effect:  $X_{corr} = -2.7$ . The predicted value of  $R_b$  is then still some  $2\sigma$  below the measured number.

Another possibility is that the charge 2/3 quark observed by CDF is in fact the  $t'$ , while the real  $t$ -quark is much lighter, say  $m_t \sim 100$  GeV. Assuming small  $t$ - $t'$  mixing,

and that the  $t'$  is the lightest member of the new multiplet, the  $t'$  will then decay to  $Wb$ , as observed by CDF, but the SM radiative correction will be reduced. This situation is essentially identical to that discussed above, in which the LH  $t$ - $t'$  mixing is maximal, and  $m_{t'} \sim 100$  GeV: the SM value of  $R_b$  will still differ from the experimental measurement by about  $2\sigma$ . The only way for such a scenario to work is if  $m_t < M_W$ . However, new physics is then once again required to evade the constraint from Ref. [24].

For all the possibilities of this section our conclusion is therefore the same: it is not possible to completely explain  $R_b$  through  $t$ - $t'$  mixing. The best we can do is reduce the discrepancy between theory and experiment to about  $2\sigma$ , which might turn out to be sufficient, depending on future measurements.

## 5. One-Loop Effects: Other Models

Another way to change  $g_L^b$  at the one-loop level is to introduce exotic new particles that couple to both the  $Z$  and the  $b$  quark. One-loop graphs involving such particles can then modify the  $Z\bar{b}b$  vertex as measured at LEP and SLC. Recall once more the conclusion from Section 2: agreement with experiment requires the LH  $b$ -quark coupling,  $g_L^b$ , to get a negative correction comparable in size to the SM  $m_t$ -dependent contributions since loop-level changes to  $g_R^b$  are too small to be detectable.

In this section we first exhibit the general one-loop correction due to exotic new scalar and spin-half particles, with the goal of identifying the features responsible for the overall sign and magnitude of the result. We then use this general result to investigate a number of more specific cases.

The answer is qualitatively different depending on whether or not the new scalars and fermions can mix, and thus have off-diagonal couplings to the  $Z$  boson. We therefore treat these two alternatives separately. The simplest case is when all  $Z$  couplings are diagonal, so that the one-loop results depend only upon two masses, those of the fermion and the scalar in the loop. Then the correction to the  $Zb\bar{b}$  vertex is given by a very simple analytic formula, which enables us to easily explain why a number of models in this category give the ‘wrong’ sign, reducing  $\Gamma_b$  rather than increasing it.

More generally however, the new particles in the loops have couplings to the  $Z$  which are diagonal only in the flavour basis but not the mass eigenstate basis, so the expressions become significantly more complicated. This occurs in supersymmetric extensions of the standard model, for example. After proposing several sample models which can resolve the  $R_b$  problem, we use our results to identify which features of supersymmetric models are instrumental in so doing.

### 5.1) Diagonal Couplings to the $Z$ : General Results

We now present formulae for the correction to the  $Z\bar{b}b$  vertex due to a loop involving generic scalar and spin-half particles. In this section we make the simplifying assumption that all of the  $Z$ -boson couplings are flavour diagonal. This condition is relaxed in later sections where the completely general expression is derived. The resulting formulae make it possible to see at a glance whether a given model gives the right sign for alleviating the discrepancy between experiment and the SM prediction for  $R_b$ .

The one-loop diagrams contributing to the decay  $Z \rightarrow b\bar{b}$  can be grouped according to whether the loop attaches to the  $b$  quark (*i.e.* the vertex correction and self-energy graphs of Fig. 5) or whether the loop appears as part of the gauge boson vacuum polarization (Fig. 6). For the types of models we consider these two classes of graphs are separately gauge invariant and finite, and so they can be understood separately. This is particularly clear in the limit that the particles within the loop are heavy compared to  $M_Z$ , since then the vacuum polarization graphs represent the contribution of the oblique parameters,  $S$  and  $T$ , while the self-energy and vertex-correction graphs describe loop-induced shifts to the  $b$ -quark neutral current couplings,  $\delta g_{L,R}^b$ .

Furthermore, although we must ensure that the oblique parameters do not become larger than the bound of eq. (3), eq. (4) shows that they largely cancel in the ratio  $R_b$ . We therefore restrict our attention in this section to the diagrams of Fig. 5 by themselves. The sum of the contributions of Fig. 5 is also finite as a result of the Ward identity which was alluded to in Section 3. This Ward identity relates the vertex-part graphs of Fig. 5a,b to the self-energy graphs of Fig. 5c,d. Since this cancellation is an important check of our results, let us explain how it comes about.

We first consider an unbroken  $U(1)$  gauge boson with a tree-level coupling of  $g_b$  to the  $b$ -quark. This gives rise to the familiar Ward identity from quantum electrodynamics: for external fermions with four-momenta  $p$  and  $p'$ ,

$$(p - p')^\mu \Gamma_\mu = g_{\text{eff}}(S_F^{-1}(p) - S_F^{-1}(p')), \quad (74)$$

where  $\Gamma^\mu$  is the one-particle-irreducible vertex part and  $S_F(p)$  is the fermion propagator. If we denote the vertex-part contributions (Fig. 5a,b) to the effective vertex at zero momentum transfer by  $\delta g_b$ , and the self-energy-induced wave function renormalization of the  $b$  quark by  $Z_b$ , then at one loop the Ward identity (74) reduces to  $g_b(1 + Z_b)(\not{p} - \not{p}') = (g_b + \delta g_b)(\not{p} - \not{p}')$ , or

$$\delta g_b - g_b Z_b = 0. \quad (75)$$

This last equation is the more general context for the cancellation which we found in Section 3; it states that the self-energy graphs (Fig. 5c,d) must precisely cancel the vertex part (Fig. 5a,b) in the limit of zero momentum transfer. Another way of understanding eq. (75) is to imagine computing the effective  $b$ -photon vertex due to integrating out a heavy particle. Eq. (75) is the condition that the two effective operators  $\bar{b}\not{p}b$  and  $\bar{b}\not{A}b$  have the right relative normalization to be grouped into the gauge-covariant derivative:  $\bar{b}\not{D}b$ .

But for the external  $Z$  boson, the Ward identity only applies to those parts of the diagrams which are insensitive to the fact that the  $U(1)$  symmetry is now broken. These include the  $1/(n-4)$  poles from dimensional regularization, and also the contributions to the  $b$  neutral-current coupling proportional to  $s_w^2$ , since the latter arise only through mixing from the couplings of the photon.

We now return to the diagrams of Fig. 5. The first step is to establish the Feynman rules for the various vertices which appear. Since we care only about the LH neutral-current couplings, it suffices to consider couplings of the new particles to  $b_L$ :

$$\mathcal{L}_{\text{scalar}} = y_{f\phi} \phi \bar{f} \gamma_L b + \text{h.c.} \quad (76)$$

and we write the  $Z$  coupling to  $f$  and  $\phi$  as

$$\mathcal{L}_{\text{nc}} = \left( \frac{e}{s_w c_w} \right) Z^\mu \left[ \bar{f} \gamma_\mu (g_L^f \gamma_L + g_R^f \gamma_R) f + i g_s \phi^\dagger \overleftrightarrow{\partial}_\mu \phi \right]. \quad (77)$$

The couplings,  $g = \{g_L^f, g_R^f, g_s\}$ , are normalized so that  $g = I_3 - Q s_w^2$  for all fields,  $f_{L,R}^a$  and  $\phi^m$ .

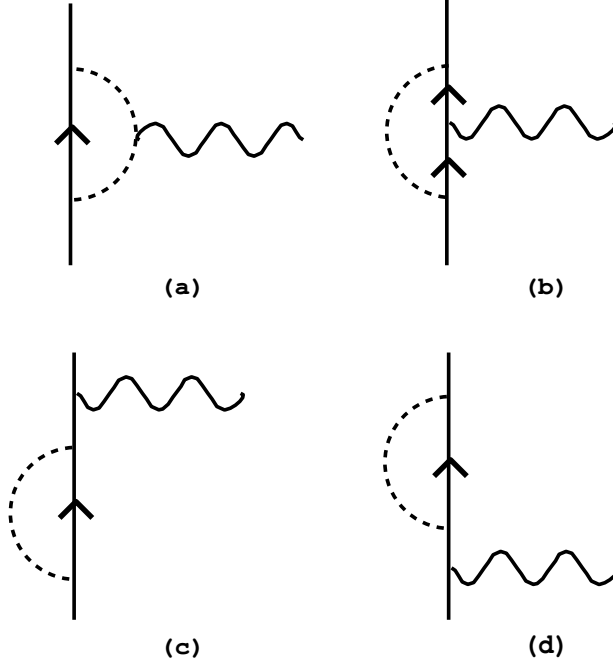


**Figure 5**

Figure 5: The one-loop vertex correction and self-energy contributions to the  $Zb\bar{b}$  vertex due to fermion-scalar loops.

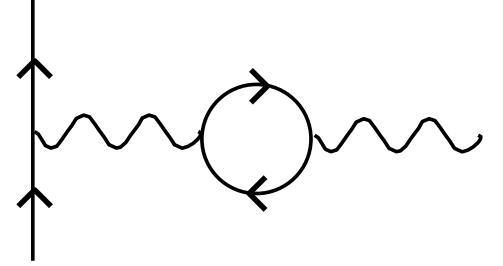


**Figure 6**

Figure 6: The one-loop contributions to the  $Zb\bar{b}$  vertex due to the gauge-boson vacuum polarizations.

In the examples which follow, the field  $f$  can represent either an ordinary spinor (*e.g.*,  $t$ ) or a *conjugate* spinor (*e.g.*,  $t^c$ ). This difference must be kept in mind when inferring the corresponding charge assignments for the neutral-current couplings of the  $f$ . For example, the left-handed top quark has  $I_{3L} = +\frac{1}{2}$ , so  $g_L^f = \frac{1}{2} - \frac{2}{3}s_w^2$  and  $I_{3R} = 0$ , so  $g_R^f = -\frac{2}{3}s_w^2$ . If the internal fermion were a top *antiquark*, however, we would instead have  $g_R^f = -\frac{1}{2} + \frac{2}{3}s_w^2$  and  $g_L^f = +\frac{2}{3}s_w^2$ . The latter couplings follow from the former using the transformation of the neutral current under charge conjugation:  $\gamma_\mu\gamma_L \leftrightarrow -\gamma_\mu\gamma_R$ .

We quote the results for evaluating the graphs of Fig. 5 in the limit where  $M_Z$  (and of course  $m_b$ ) are negligible compared to  $m_f$  and  $M_\phi$ , since they are quite simple and illuminating in this approximation. It will be shown that the additional corrections due to the nonzero mass of the  $Z$  boson are typically less than 10% of this leading contribution. We find that

$$\delta g_L^b = \frac{1}{32\pi^2} \sum_{f\phi} n_c |y_{f\phi}|^2 \left[ 2(g_L^f - g_R^f) \mathcal{F}(r) + (-g_R^f + g_L^b + g_s) (\Delta_\phi + \tilde{\mathcal{F}}(r)) \right], \quad (78)$$

where  $\mathcal{F}(r)$  and  $\tilde{\mathcal{F}}(r)$  are functions of the mass ratio  $r = m_f^2/M_\phi^2$ ,

$$\mathcal{F}(r) \equiv \frac{r}{(r-1)^2} \left[ r - 1 - \ln r \right], \quad (79)$$

$$\tilde{\mathcal{F}}(r) \equiv \frac{r}{(r-1)^2} \left[ r - 1 - r \ln r \right]. \quad (80)$$

$\Delta_\phi$  denotes the divergent combination  $\Delta_\phi \equiv \frac{2}{n-4} + \gamma + \ln(M_\phi^2/4\pi\mu^2) + \frac{1}{2}$ , and  $n_c$  is a colour factor that depends on the  $SU_c(3)$  quantum numbers of the fields  $\phi$  and  $f$ . For example,  $n_c = 1$  if  $\phi \sim \mathbf{1}$  or  $f \sim \mathbf{1}$  (colour singlets);  $n_c = 2$  if  $f \sim \bar{\mathbf{3}}$  and  $\phi \sim \bar{\mathbf{3}}$  or  $\mathbf{6}$ ;  $n_c = \frac{16}{3}$  if  $f \sim \mathbf{3}$  and  $\phi \sim \mathbf{8}$ .

The cancellation of divergences we expected on general grounds is now evident in the present example, because electroweak gauge invariance of the scalar interaction (76) implies that the neutral-current couplings are related by

$$g_S + g_L^b - g_R^f = 0. \quad (81)$$

This forces the term proportional to  $\tilde{\mathcal{F}}$  to vanish in eq. (78). As advertised the remaining term is both ultraviolet finite and independent of  $s_w^2$ , which cancels in the combination  $g_L^f - g_R^f$ .

We are left with the compact expression

$$\delta g_L^b = \frac{1}{16\pi^2} \sum_{f\phi} n_c |y_{f\phi}|^2 (g_L^f - g_R^f) \mathcal{F}(m_f^2/M_\phi^2). \quad (82)$$

Interestingly, it depends only on the axial-vector coupling of the internal fermion to the gauge boson  $W_3$  and not on the vector coupling. The function of the masses  $\mathcal{F}(r)$  is positive and monotonically increasing, with  $\mathcal{F}(r) \sim r$  as  $r \rightarrow 0$  and  $\mathcal{F}(\infty) = 1$ , as can be seen in Fig. 7.

It is straightforward to generalize eq. (82) to include the effect of the nonzero  $Z$  boson mass. Expanding to first order in  $M_Z^2$ , one obtains an additional correction to the effective vertex,

$$\delta_Z g_L^b = \sum_{f\phi} \frac{|y_{f\phi}|^2 n_c}{96\pi^2} \left( \frac{M_Z^2}{m_f^2} \right) \int_0^1 dx \left\{ \frac{x^3 (g_L^b - g_R^f) + 2(1-x)^3 g_R^f}{x(M_\phi^2/m_f^2 - 1) + 1} + \frac{(1-x)^3 g_L^f}{(x(M_\phi^2/m_f^2 - 1) + 1)^2} \right\}. \quad (83)$$

To see that this is typically an unimportant correction, consider the limit in which the scalar and fermion masses are equal,  $r = 1$ . Then the total correction (82)+(83) is

$$\delta g_L^b + \delta_Z g_L^b = \sum_{f\phi} \frac{|y_{f\phi}|^2 n_c}{32\pi^2} \left( g_L^f - g_R^f + \frac{M_Z^2}{12 m_f^2} (g_L^b + g_L^f + g_R^f) \right). \quad (84)$$

Although the  $M_Z^2$  correction can be significant if  $g_L^f = g_R^f$ , the total correction would then be too small to explain the  $R_b$  discrepancy, and would thus be irrelevant.

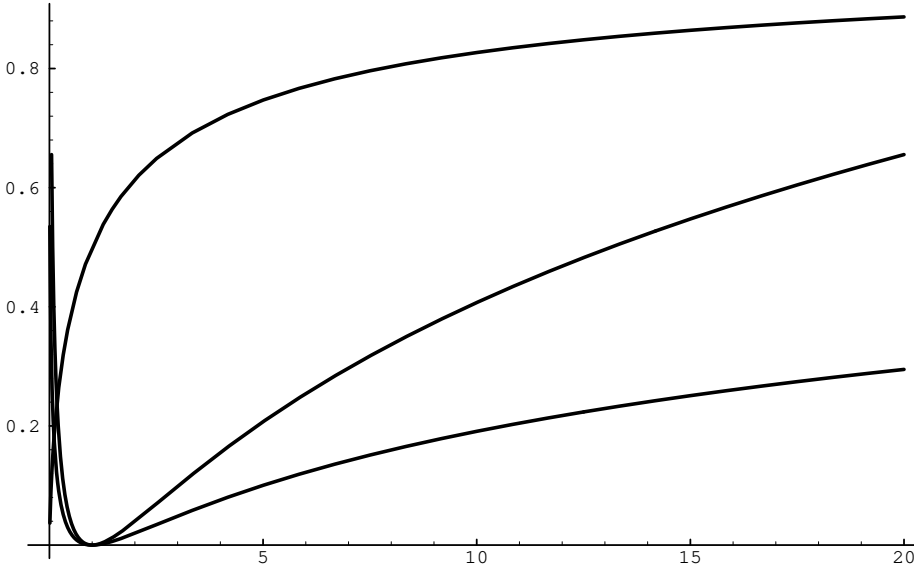


Figure 7: From top to bottom, the functions  $\mathcal{F}(m_f^2/M_\phi^2)$ ,  $F_R(r) = F_S(r)$  and  $F_L(r)$  which appear in the loop contribution to the left-handed  $Zb\bar{b}$  vertex, sections 5.1 and 5.3.

## 5.2) Why Many Models Don't Work

What is important for applications is the relative sign between the tree and one-loop contributions of eq. (82). In order to increase  $R_b$  so as to agree with the experimental observation, one needs for them both to have the same sign, and so  $\delta g_L^b \propto (g_L^f - g_R^f) < 0$  in eq. (82). Thus an internal fermion with the quantum numbers of the  $b$ -quark has  $g_L^f - g_R^f = -\frac{1}{2}$  and would increase  $R_b$ . Conversely, a fermion like the  $t$ -quark has  $g_L^f - g_R^f = +\frac{1}{2}$  and so causes a decrease. Moreover, because the combination  $(g_L - g_R)$  is invariant under charge conjugation, the same statements hold true for the antiparticles: a  $\bar{b}$  running in the loop would increase  $R_b$  whereas a  $\bar{t}$  would decrease it.



It thus becomes quite easy to understand which models with diagonal couplings to the  $Z$  boson can improve the prediction for  $R_b$ . Multi-Higgs-doublet models have a hard time explaining an  $R_b$  excess because typically it is the top quark that makes the dominant contribution to the loop diagram, since it has the largest Yukawa coupling,  $y_{f\phi} \sim 1$ , and the largest mass, to which the function  $\mathcal{F}$  is very sensitive. However for very small  $\tan\beta$  (the ratio of the two Higgs VEV's), the Yukawa coupling of the  $t$  quark to the charged Higgs can be made small and that of the  $b$  quark can be made large, as in Ref. [25]. Fig. 7 shows that, in fact, one must go to extreme values of these parameters, because in addition to needing to invert the natural hierarchy between  $y_t$  and  $y_b$ , one must overcome the big suppression for small fermion masses coming from the function  $\mathcal{F}$ .

Precisely the same argument applies to a broad class of Zee-type models, where the SM is supplemented by scalar multiplets whose weak isospin and hypercharge permit a Yukawa coupling to the  $b$  quark and one of the other SM fermions. So long as the scalars do not mix and there are no new fermions to circulate in the loop, all such models have the same difficulty in explaining the  $R_b$  discrepancy. Below we will give some examples of models which, in contrast, *are* able to explain  $R_b$ .

### 5.3) Generalization to Nondiagonal $Z$ Couplings

We now turn to the more complicated case where mixing introduces off-diagonal couplings among the new particles. Because of mixing the couplings of the fermions to the  $Z$  will be matrices in the mass basis. Similar to eqs. (42) and (45) we write

$$(g_{L,R})^{ff'} = \sum_a \left[ (\mathcal{U}_{L,R}^{af})^* \mathcal{U}_{L,R}^{af'} I_{3L,R}^a - \delta^{ff'} Q^a s_w^2 \right], \quad (85)$$

where  $\mathcal{U}_{L,R}^{af}$  are the mixing matrices. An analogous expression gives the off-diagonal scalar- $Z$  coupling in terms of the scalar mixing matrix,  $\mathcal{U}_S^{a\phi}$ . Of course if all of the mixing particles share the same value for  $I_3$ , then unitarity of the mixing matrices guarantees that the couplings retain this form in any basis.

This modification of the neutral-current couplings has two important effects on the calculation of  $\delta g_L^b$ . One is that the off-diagonal  $Z$  couplings introduce the additional graphs of the type shown in Fig. 5a,b, where the fermions or scalars on either side of the  $Z$  vertex have different masses. The other is that the mixing matrices spoil the relationship, eq. (81), whereby the term proportional to  $\tilde{\mathcal{F}}$  canceled in eq. (78). But this is only because of the mass-dependence of  $\mathcal{F}$  and  $\Delta_\phi$ . Therefore the cancellation still occurs if all of the particles

that mix with each other are degenerate, as one would expect. Moreover the ultraviolet divergences still cancel since they are mass-independent.

Evaluation of the graphs gives the following result at  $q^2 = M_Z^2 = 0$ :

$$\delta g_L^b = \frac{1}{32\pi^2} \left[ G_{\text{diag}} + G_{ff'} + G_{\phi\phi'} \right], \quad (86)$$

where  $G_{\text{diag}}/32\pi^2$  represents the contribution involving only the diagonal  $Z$  couplings, and so is identical to the previously derived eq. (78). It is convenient to write it as

$$G_{\text{diag}} = \sum_{f\phi} n_c |y_{f\phi}|^2 \left\{ 2(g_L - g_R)^{ff} \mathcal{F}(r) + \left[ -(g_R)^{ff} + g_L^b + (g_S)^{\phi\phi} \right] \left( \Delta_\phi + \tilde{\mathcal{F}}(r) \right) \right\}. \quad (87)$$

Here and in the following expressions we use the notation  $r = m_f^2/M_\phi^2$  and  $r' = m_{f'}^2/M_\phi^2$ . As before  $\Delta_\phi$  denotes the UV-divergent quantity  $\Delta_\phi \equiv \frac{2}{n-4} + \gamma + \ln(M_\phi^2/4\pi\mu^2) + \frac{1}{2}$ .

The remaining terms in eq. (86) come from the new graphs of Fig. 5a,b, where the scalars or fermions on either side of the  $Z$  vertex have different masses, due to mixing:

$$G_{ff'} = \sum_{\phi, f \neq f'} n_c y_{f\phi} y_{f'\phi}^* \left[ 2(g_L)^{ff'} \mathcal{F}_L(r, r') - (g_R)^{ff'} \left( \Delta_\phi + \mathcal{F}_R(r, r') \right) \right], \quad (88)$$

$$G_{\phi\phi'} = \sum_{f, \phi \neq \phi'} n_c y_{f\phi} y_{f\phi'}^* (g_S)^{\phi\phi'} \left[ \Delta_\phi + \mathcal{F}_S(x, x') \right], \quad (89)$$

where  $\mathcal{F}_L(r, r')$ ,  $\mathcal{F}_R(r, r')$  and  $\mathcal{F}_S(x, x')$  are given by:

$$\mathcal{F}_L(r, r') = \frac{\sqrt{rr'}}{r - r'} \left[ \frac{r}{r - 1} \ln r - \frac{r'}{r' - 1} \ln r' \right], \quad (90)$$

$$\mathcal{F}_R(r, r') = \frac{1}{r - r'} \left[ \frac{r^2}{r - 1} \ln r - \frac{r'^2}{r' - 1} \ln r' \right], \quad (91)$$

$$\mathcal{F}_S(x, x') = \frac{1}{(x - 1)(x' - 1)} \left( 1 + \ln x \right) + \frac{x'^2}{(x' - 1)(x' - x)} \left( 1 + \ln \frac{x}{x'} \right) + \frac{x^2}{(x - 1)(x - x')}, \quad (92)$$

and  $x, x'$  are the mass ratios  $x = M_\phi^2/m_f^2$  and  $x' = M_\phi^2/m_{f'}^2$ . These expressions have several salient features which we now discuss. First, eqs. (87), (88) and (89) are obviously much more complicated than eq. (82). In particular, it is no longer straightforward to simply read off the sign of the result.

Second, the sum of the UV divergences in eqs. (87), (88) and (89),

$$G_\Delta \propto \sum_{ff'\phi\phi'} y_{f\phi} y_{f'\phi'}^* \left[ -(g_R)^{ff'} \delta^{\phi\phi'} + g_L^b \delta^{ff'} \delta^{\phi\phi'} + (g_S)^{\phi\phi} \delta^{ff'} \right], \quad (93)$$

is *basis independent* since a unitary transformation of the fields cancels between the Yukawa and neutral-current couplings. Thus it can be evaluated in the electroweak basis where the neutral-current couplings are diagonal and proportional to  $-g_R^f + g_L^b + g_S$ , which vanishes due to conservation of weak isospin and hypercharge at the scalar-fermion vertex. We are therefore free to choose the renormalization scale  $\mu^2$  in  $\ln(M_\phi^2/\mu^2)$  to take any convenient value. The  $M_\phi$ -dependence of  $\Delta_\phi$  makes  $G_{\phi\phi'}$  look unsymmetric under the interchange of  $\phi$  and  $\phi'$ , but this is only an artifact of the way it is expressed. For example when there are only two scalars,  $G_{\phi\phi'}$  is indeed symmetric under the interchange of their masses.

Third, all the contributions *except* those of  $G_{\phi\phi'}$  are suppressed by powers of  $m_f/M_\phi$  in the limit that the scalars are much heavier than the fermions. Thus to get a large enough correction to  $g_L^b$  requires that: (i) not all of the scalars be much heavier than the fermions which circulate in the loop, or (ii) the scalars mix significantly and have the right charges so that  $G_{\phi\phi'}$  is nonnegligible and negative. We use option (ii) in what follows to construct another mechanism for increasing  $R_b$ .

Finally, even if the two fermions are degenerate, one does not generally recover the previous expression (78) that applied in the absence of mixing. This is because Dirac mass matrices are diagonalized by a similarity transformation,  $M \rightarrow \mathcal{U}_L^\dagger M \mathcal{U}_R$ , not a unitary transformation. The left- and right-handed mixing angles can differ even when the diagonalized mass matrix is proportional to the identity. Thus, in contrast to eq. (93), the expression  $\sum_{ff'\phi\phi'} y_{f\phi} y_{f'\phi'}^* [(g_L)^{ff'} - (g_R)^{ff'}]$  is not invariant under transformations of the fields, because  $y_{f\phi}$  is rotated by  $\mathcal{U}_R$  (recall that  $y_{f\phi}$  is the Yukawa coupling only for the RH  $f$ 's) whereas  $g_L$  is rotated by  $\mathcal{U}_L$ .

We can get some insight into eqs. (88)–(92) by looking at special values of the parameters. Let us assume there is a dominant Yukawa coupling  $y$  between the left-handed  $b$  quark and a single species of scalar and fermion,  $f_1$  and  $\phi_1$  in the weak basis,

$$\mathcal{L}_{\text{scalar}} = y \phi_1 \bar{f}_1 \gamma_L b + \text{h.c.} \quad (94)$$

In the mass basis the couplings will therefore be

$$y_{f\phi} = y \mathcal{U}_S^{1\phi} (\mathcal{U}_R^{1f})^*. \quad (95)$$

Now gauge invariance only relates the  $(1, 1)$  elements of the neutral-current coupling matrices in the weak basis:

$$(g_S)^{11} + g_L^b - (g_R^f)^{11} = 0. \quad (96)$$

There are three limiting cases in which the results become easier to interpret:

- 1: If all the scalars are degenerate with each other, and likewise for the fermions, then the nonmixing result of eq. (82) holds, except one must make the replacement

$$g_L^f - g_R^f \rightarrow (\mathcal{U}_R S_m \mathcal{U}_L^\dagger g_L \mathcal{U}_L S_m \mathcal{U}_R^\dagger - g_R)^{11}, \quad (97)$$

where  $S_m$  is the diagonal matrix of the signs of the fermion masses,  $S_m = \text{diag}(m_f, m_{f2}, \dots) / |m_f|$ .

- 2: If there are only two scalars and if they are much heavier than all of the fermions, only the term  $G_{\phi\phi'}$  is significant. Let  $\phi_1$  and  $\phi_2$  denote the weak-eigenstate scalars, and  $\phi$  and  $\phi'$  the mass eigenstates; then

$$\delta g_L^b = \frac{y^2 n_c}{16\pi^2} (I_3^{\phi_2} - I_3^{\phi_1}) c_S^2 s_S^2 F_S(M_\phi^2/M_{\phi'}^2); \quad (98)$$

$$F_S(r) = \frac{r+1}{2(r-1)} \ln r - 1, \quad (99)$$

where  $c_S$  and  $s_S$  are the cosine and sine of the scalar mixing angle. The function  $F_S(r)$  is positive except at  $r = 1$  where it is zero, and so the sign of  $\delta g_L^b$  is completely controlled by the factor  $(I_3^{\phi_2} - I_3^{\phi_1})$ . We see that to increase  $R_b$  it is necessary that  $I_3^{\phi_1} > I_3^{\phi_2}$ .

- 3: When there are only two fermions, with weak eigenstates  $f_1, f_2$  and mass eigenstates  $f, f'$  both much heavier than any of the scalars, then

$$\begin{aligned} \delta g_L^b = \frac{y^2 n_c}{16\pi^2} \bigg\{ & g_L^{11} c_{LR}^2 + g_L^{22} s_{LR}^2 - g_R^{11} \\ & + (g_R^{22} - g_R^{11}) c_R^2 s_R^2 F_R(m_f^2/m_{f'}^2) - 2(g_L^{22} - g_L^{11}) c_L s_L c_R s_R F_L(m_f^2/m_{f'}^2) \bigg\}; \end{aligned} \quad (100)$$

where  $s_{LR}$  and  $c_{LR}$  are the sine and cosine of the difference or sum of the LH and RH mixing angles,  $\theta_L - s_m \theta_R$ , depending on the relative sign  $s_m$  of the two fermion mass eigenvalues, and

$$F_R(r) = F_S(r) = \frac{r+1}{2(r-1)} \ln r - 1; \quad \text{and} \quad F_L(r) = \frac{\sqrt{r}}{r-1} \ln r - 1. \quad (101)$$

The function  $F_L$  has some of the same properties as  $F_S = F_R$ , including invariance under  $r \rightarrow 1/r$ , being positive semidefinite and vanishing at  $r = 1$ . Plots of these functions are shown in Figure 7. Note that the first line of eq. (100) is the same as (96).

To get some idea of the error we have made by neglecting the mass of the  $Z$  boson one can compute the lowest order correction as in section 5.3. The answer is more complicated than for the case of diagonal  $Z$  couplings, except when the fermions are degenerate with each other and likewise for the bosons. In that case the answer is given again by eq. (84) except that  $g_R^f \rightarrow (g_R^f)^{11}$  and  $g_L^f \rightarrow (\mathcal{U}_R S_m \mathcal{U}_L^\dagger g_L \mathcal{U}_L S_m \mathcal{U}_R^\dagger - g_R)^{11}$ , precisely as in eq. (97). Thus we would still expect it to be a small correction even when there is mixing of the particles in the loop.

These simplifying assumptions can be used to gain a semi-analytic understanding of why certain regions of parameter space are favoured in complicated models, which is often missing in analyses that treat the results for the loop integrals as a black box. The observations we make here may be useful when searching for modifications to a model that would help to explain  $R_b$ . The next two sections exemplify this by creating some new models that take advantage of our insights, and by elucidating previous findings in an already existing model, supersymmetry.

#### 5.4) Examples of Models That Work

Besides ruling out certain classes of models, our general considerations also suggest what *is* required in order to explain  $R_b$ . Obviously new fermions and scalars are required, whose Yukawa couplings allow them to circulate inside the loop. We give two examples, one with diagonal and one with nondiagonal couplings of the new particles to the  $Z$  boson.

For our first example we introduce several exotic quarks  $F$ ,  $P$  and  $N$ , and a new Higgs doublet  $\phi$ , whose quantum numbers are listed in Table 5. The unorthodox electric charge assignments do not ensure cancellation of electroweak anomalies, but this can be fixed by adding additional fermions, like mirrors of those given, which do not contribute to  $R_b$ .

The hypercharges in Table 5 allow the following Yukawa interactions:

$$\mathcal{L}_y = y \bar{N}_R Q_L^i \phi^j \epsilon_{ij} + g_p \bar{P}_R F_L^i H^j \epsilon_{ij} + g_n \bar{N}_R F_L^i \tilde{H}^j \epsilon_{ij} + \text{h.c.}, \quad (102)$$

where  $\epsilon_{ij}$  is the  $2 \times 2$  antisymmetric tensor,  $H$  is the usual SM Higgs doublet and  $Q_L = \begin{pmatrix} t_L \\ b_L \end{pmatrix}$  is the SM doublet of third generation LH quarks. When  $H$  gets its VEV,  $\langle H \rangle = v$ , we find two fermion mass eigenstates,  $p$  and  $n$ , whose masses are  $m_p = g_p v$  and  $m_n = g_n v$

Field	Spin	$SU_c(3)$	$SU_L(2)$	$U_Y(1)$
$\phi$	0	<b>1</b>	<b>2</b>	$q - \frac{1}{6}$
$F_L$	$\frac{1}{2}$	<b>3</b>	<b>2</b>	$q + \frac{1}{2}$
$P_R$	$\frac{1}{2}$	<b>3</b>	<b>1</b>	$q + 1$
$N_R$	$\frac{1}{2}$	<b>3</b>	<b>1</b>	$q$

**Table 5**

Field Content and Charge Assignments: Electroweak quantum numbers for the new fields which are added to the SM to produce the observed value for  $R_b$ .

and whose electric charges are  $Q_p = q + 1$  and  $Q_n = q$ . There are also two new scalar mass eigenstates,  $\varphi_{\pm}$ , whose electric charges are  $Q_+ = q + \frac{1}{3}$  and  $Q_- = q - \frac{2}{3}$ .

In the mass eigenstate basis, the Yukawa interactions with the new scalars are

$$\mathcal{L}_y = y \bar{n}_R b_L \varphi_+ - y \bar{n}_R t_L \varphi_- + \text{h.c.}, \quad (103)$$

from which we see that the  $n$  couples to the  $b$ -quark as in eq. (76).

The weak isospin assignments of the  $n$  are  $I_{3L}^n = -\frac{1}{2}$  and  $I_{3R}^n = 0$ , so that  $g_L^n - g_R^n = -\frac{1}{2}$ . Therefore, from eq. (82), one obtains  $\delta g_L^b < 0$ . The central value of  $R_b$  can be reproduced if  $\delta g_L^b = -0.0067$ , which is easily obtained by taking  $y \sim 1$  and  $r \gg 1$ , so that  $\mathcal{F}(r) \simeq 1$ . The Yukawa coupling could be made smaller by putting the new scalars in a higher colour representation like the adjoint.

We have not explored the detailed phenomenology of this model, but it is clearly not ruled out since we are free to make the new fermions and scalars as heavy as we wish. And since we can always take  $m_p = m_n$ , there is no contribution to the oblique parameter  $T$ . The contribution to  $R_b$  does not vanish even as the masses become infinite, but this is consistent with decoupling in the same way as a heavy  $t$  quark, since the new fermions get their masses through electroweak symmetry breaking. The price we have to pay for such large masses is correspondingly large coupling constants.

Next we build a model that uses our results for nondiagonal couplings to the  $Z$ . It is a simple modification of the SM that goes in the right direction for fixing the  $R_b$  discrepancy but not quite far enough in magnitude. Variations on the same theme can completely explain  $R_b$  at the cost of making the model somewhat more baroque.

Our starting point is a two-Higgs doublet extension of the SM. We take the two Higgs fields,  $H_u = \begin{pmatrix} H_u^0 \\ H_u^- \end{pmatrix}$  and  $H_d = \begin{pmatrix} H_d^+ \\ H_d^0 \end{pmatrix}$ , to transform in the usual way under the SM gauge symmetry. It was explained earlier why this model does not by itself produce the desired effect, but eq. (98) suggests how to fix this problem by introducing a third scalar doublet,  $\Delta = \begin{pmatrix} \Delta^{++} \\ \Delta^+ \end{pmatrix}$ , which mixes with the other Higgs fields. The charge assignments of these fields, listed in Table 6, ensure that the two fields  $H_d^+$  and  $\Delta^+$  can mix even though they have different eigenvalues for  $I_3$ .

Field	Spin	$SU_c(3)$	$SU_L(2)$	$U_Y(1)$
$H_u$	0	<b>1</b>	<b>2</b>	$-\frac{1}{2}$
$H_d$	0	<b>1</b>	<b>2</b>	$+\frac{1}{2}$
$\Delta$	0	<b>1</b>	<b>2</b>	$+\frac{3}{2}$

**Table 6**

Field Content and Charge Assignments: Electroweak quantum numbers for all of the scalars — including the SM Higgs doublet — of the three-doublet model.

In this model the new scalar field cannot have any Yukawa couplings to ordinary quarks since these are forbidden by hypercharge conservation. The only Yukawa couplings involving the  $b$ -quark are those which also generate its mass:

$$\mathcal{L}_{yuk} = y_b \sqrt{2} \bar{t} \gamma_L b H_d^+ + \text{h.c.}, \quad (104)$$

where  $y_b = m_b/v_d$  is the conventionally-normalized Yukawa coupling. We imagine  $v_d$  to be as small as is possible in order to enhance  $y_b$ . For such choices  $v_u$  approaches the single-Higgs SM value, and so we expect  $y_t$  to be comparable to its SM size.

The scalar potential for such a model very naturally incorporates  $H_d^+ - \Delta^+$  mixing. Gauge invariance permits quartic scalar interactions of the form  $\lambda(H_d^\dagger \Delta)(H_d^\dagger H_u) + \text{h.c.}$ , which generate the desired off-diagonal terms:  $\lambda(\Delta^+ H_d^{+*} v_d^* v_u + \Delta^+ H_u^- v_d^{2*}) + \text{h.c.}$

Since the weak isospin assignments are  $I_3^{\Delta^+} = -\frac{1}{2}$  and  $I_3^{H_d^+} = +\frac{1}{2}$ , the colour factor is  $n_c = 1$  and the relevant Yukawa coupling is  $y = y_b \sqrt{2}$ , we see that eq. (98) predicts the

following contribution due to singly-charged Higgs loops:

$$\delta g_L^b = -\frac{y_b^2}{16\pi^2} 2c_s^2 s_s^2 F_s(r) , \quad (105)$$

with  $r$  being the ratio of the scalar mass eigenstates,  $r = M_\phi^2/M_{\phi'}^2$ . Taking optimistic values for the parameters<sup>12</sup> ( $\theta_s = \frac{\pi}{4}$ ,  $2c_s^2 s_s^2 = \frac{1}{2}$ ,  $y_b = 1$  and  $M_\phi/M_{\phi'} = 10$ ), we find  $\delta g_L^b = -0.0043$ , which is two thirds of what is required:  $(\delta g_L^b)_{\text{exp}} = -0.0067 \pm 0.0021$ .

In addition to the contribution of the singly-charged scalar loops, one should consider those of the other nonstandard scalar fields we introduced. Since all of the scalars that mix have the same eigenvalue for  $I_3$ , their contribution is given by eq. (82), which is small if the scalars are much heavier than the light fermions. Then only the  $t$ -quark contribution is important. In this limit there are appreciable contributions only from the three charged scalar fields, one of which is eaten by the physical  $W$  boson and so is incorporated into the SM  $t$ -quark calculation, and the other two of which we have just computed.

So, for an admittedly special region of parameter space, this simple model considerably ameliorates the  $R_b$  discrepancy, reducing it to a  $1\sigma$  effect. It is easy to adapt it so as to further increase  $\delta g_L^b$  and also enlarge the allowed region of the model's parameter space. The simplest way is by increasing the size of the colour factor  $n_c$  or the isospin difference  $I_3^{\phi'} - I_3^\phi$ . For instance the new scalar,  $\Delta$ , could be put into a **4** of  $SU_L(2)$  rather than a doublet, and be given weak hypercharge  $Y = +\frac{5}{2}$ . Then the singly-charged state  $\Delta^+$  has  $I_3^{\Delta^+} = -\frac{3}{2}$ , making  $I_3^{\phi'} - I_3^\phi = -2$ , which is twice as big as for the doublet. More new scalars must be added to generate mixing amongst the singly-charged scalar states.

A second variation would be let the two new Higgs doublets be colour octets since this gives more than a five-fold enhancement of  $\delta g_L^b$  due to the colour factor  $n_c = \frac{16}{3}$ . It is still possible to write down quartic scalar interactions which generate the desired scalar mixings. Either of these models has much more room to relax the previously tight requirements for optimal scalar masses and mixings.

### 5.5) The Supersymmetric Case

Let us now apply the above results to gain some insight into what would be necessary to explain  $R_b$  in supersymmetric extensions of the standard model. There are two kinds of contributions involving the top-quark Yukawa coupling, which one expects to give the

---

<sup>12</sup> Note that the charged-scalar mixing in this model is suppressed if one of the scalar masses gets very large compared to the weak scale.



dominant effect. These are the couplings of the left-handed  $b$  quark to the second Higgs doublet and the top quark, or to the corresponding Higgsinos and top squarks,

$$y_t \bar{b}_L \tilde{h}_{2,R}^- \tilde{t}_R + y_t \bar{b}_L t_R h_2^-. \quad (106)$$

Of these, the second one gives a loop contribution like that of the two-Higgs doublet models discussed above: it has the wrong sign for explaining  $R_b$ . Since the mass of the charged Higgs is a free parameter in supersymmetric models, we can imagine making it large enough compared to  $m_t$  so that, according to eq. (82), it has only a small effect on  $R_b$ . We therefore concentrate on the Higgsino-squark part. The charged Higgsino mixes with the Wino, and the right-handed top squark mixes with its chiral counterpart, so in the notation of (94), we have  $f_1 = \tilde{h}_2^-$ ,  $f_2 = \tilde{W}^-$ ,  $\phi_1 = \tilde{t}_R$  and  $\phi_2 = \tilde{t}_L$ . The corresponding charge matrices for the couplings to the  $W_3$  are

$$g_S = \begin{pmatrix} \frac{2}{3}s_w^2 & 0 \\ 0 & \frac{1}{2} + \frac{2}{3}s_w^2 \end{pmatrix}; \quad g_L = g_R = \begin{pmatrix} -\frac{1}{2} - s_w^2 & 0 \\ 0 & -1 - s_w^2 \end{pmatrix}. \quad (107)$$

Because there are two possible colour combinations for the internal lines of the loops diagram, the colour factor in eqs. (87)-(89) is  $n_c = 2$ .

Before exploring the full expression for  $\delta g_L^b$  we can discover what parameter ranges are the most promising by looking at the limiting cases described by eqs. (97)-(100). The most important lessons from these approximations follow from the charge matrices (107). We do not want the squarks to be much heavier than the charginos because then eq. (98) would apply and give the wrong sign for the correction due to the sign of the isospin difference between the squarks. The other two cases, where the squarks are not much heavier than the charginos, manifest a strong suppression of the result unless the chargino mixing angles are such that  $\sin(\theta_L - s_m \theta_R)$  is large, where  $s_m$  is the sign of the determinant of the chargino mass matrix. If on the other hand  $\sin(\theta_L - s_m \theta_R) = 0$ , there is exact cancellation between  $g_L$  and  $g_R$  in these equations because of the fact that  $g_L = g_R$  for the charginos. In summary, our analytic formulas indicate that the favoured regions of parameter space for increasing  $R_b$  are where

$$\tan \theta_R \tan \theta_L = -s_m = -\text{sign}(m_f m_{f'}), \quad (108)$$

and at least one of the squarks is not much heavier than the charginos.

In supersymmetric models the Yukawa coupling that controls the largest contribution to  $R_b$  is that of the top quark, and it depends on the ratio of the two Higgs VEV's,

$\tan \beta = v_2/v_1$ , by

$$y_{f\phi} = \frac{m_t}{v \sin \beta}, \quad (109)$$

where  $v = (v_1^2 + v_2^2)^{1/2} = 174$  GeV. Therefore it is important to find  $\tan \beta$  in terms of the chargino masses and mixing angles. The chargino mass matrix is given by

$$\begin{pmatrix} \mu & gv_2 \\ gv_1 & M_2 \end{pmatrix} = \mathcal{U}_L^\dagger \begin{pmatrix} m_f & 0 \\ 0 & m_{f'} \end{pmatrix} \mathcal{U}_R = \begin{pmatrix} c_L c_R m_f + s_L s_R m_{f'} & s_R c_L m_f - c_R s_L m_{f'} \\ c_R s_L m_f - s_R c_L m_{f'} & s_L s_R m_f + c_L c_R m_{f'} \end{pmatrix}, \quad (110)$$

where  $\mu$  is the coefficient of  $H_1 H_2$  in the superpotential and  $M_2$  is the soft-SUSY-breaking mass term for the Wino. It follows that

$$\tan \beta = \frac{m_f \tan \theta_R - m_{f'} \tan \theta_L}{m_f \tan \theta_L - m_{f'} \tan \theta_R} \quad (111)$$

The above considerations allow us to understand why values of  $\tan \beta$  near unity are necessary for a supersymmetric solution to the  $R_b$  problem. From eq. (111) and the maximization condition (108) we see that  $\tan \beta$  is restricted to lie between  $|m_f/m_{f'}|$  and  $|m_{f'}/m_f|$ . Eq. (108) together with (110) also implies

$$c_L^2 |m_f| + s_L^2 |m_{f'}| = \sqrt{2} M_W \sin \beta; \quad c_L^2 |m_{f'}| + s_L^2 |m_f| = \sqrt{2} M_W \cos \beta, \quad (112)$$

This means that average value of the two chargino masses can be no greater than  $M_W$ , so that the ratio  $|m_f/m_{f'}|$  cannot differ much from unity unless one of the charginos is much lighter than the  $W$  boson. Using the LEP 1.5 limit of 65 GeV for the lightest chargino [26] this would then require that  $\tan \beta < 1.5$ .

In the case that none of our simplifying limits apply, we have searched the parameter space of the three independent ratios between the two scalar masses and the two fermion masses, and the three mixing angles  $\theta_R$ ,  $\theta_L$ ,  $\theta_S$  to find which regions are favourable for increasing  $R_b$ . Figures 8a-d show the shift in  $g_L^b$  as a function of pairs of these parameters, using the Yukawa coupling (109) corresponding to a top quark mass of 174 GeV and the theoretical preference for  $\tan \beta > 1$  (we implement the latter by setting  $g_L^b = 0$  for parameters that would give  $\tan \beta < 1$ ). As shown in Table 1, one needs  $g_L^b = -0.0067$  in order to explain the observed value of  $R_b$ . The values of the masses are taken to be  $M_\phi \cong M_{\phi'} \cong m_f \cong m_{f'} = 1$  (in arbitrary units), except for those that are explicitly varied in each figure. In Fig. 8a we look at the situation in which  $\tan \theta_L = \tan \theta_R = 1$ , in contradiction to condition (108), and vary the scalar mixing angle and one of the scalar

masses. The sign of  $g_L^b$  has the wrong value, as predicted by eq. (98). Fig. 8b shows the same situation except that now  $\tan \theta_L = -\tan \theta_R = 1$ , in accordance with eq. (108). Then the sign of  $g_L^b$  is negative, as desired, and has the right size for substantial ranges of  $\theta_s$  and  $M_\phi$ . In Fig. 8c we keep all the masses nearly degenerate and set  $\theta_s = 0$  to show the dependence on  $\tan \theta_L$  and  $\tan \theta_R$ . It is easy to see that  $g_L^b$  has the correct sign and largest magnitude (which is also almost as large as needed) when condition (108) is satisfied. Finally in Fig. 8d we show the dependence on one of the fermion masses and on  $\theta_R$  when  $\theta_s = 0$  and  $\tan \theta_L = -1$ , showing again the preference for mixing angles obeying (108), as well as some enhancement when there is a hierarchy between the two chargino masses.

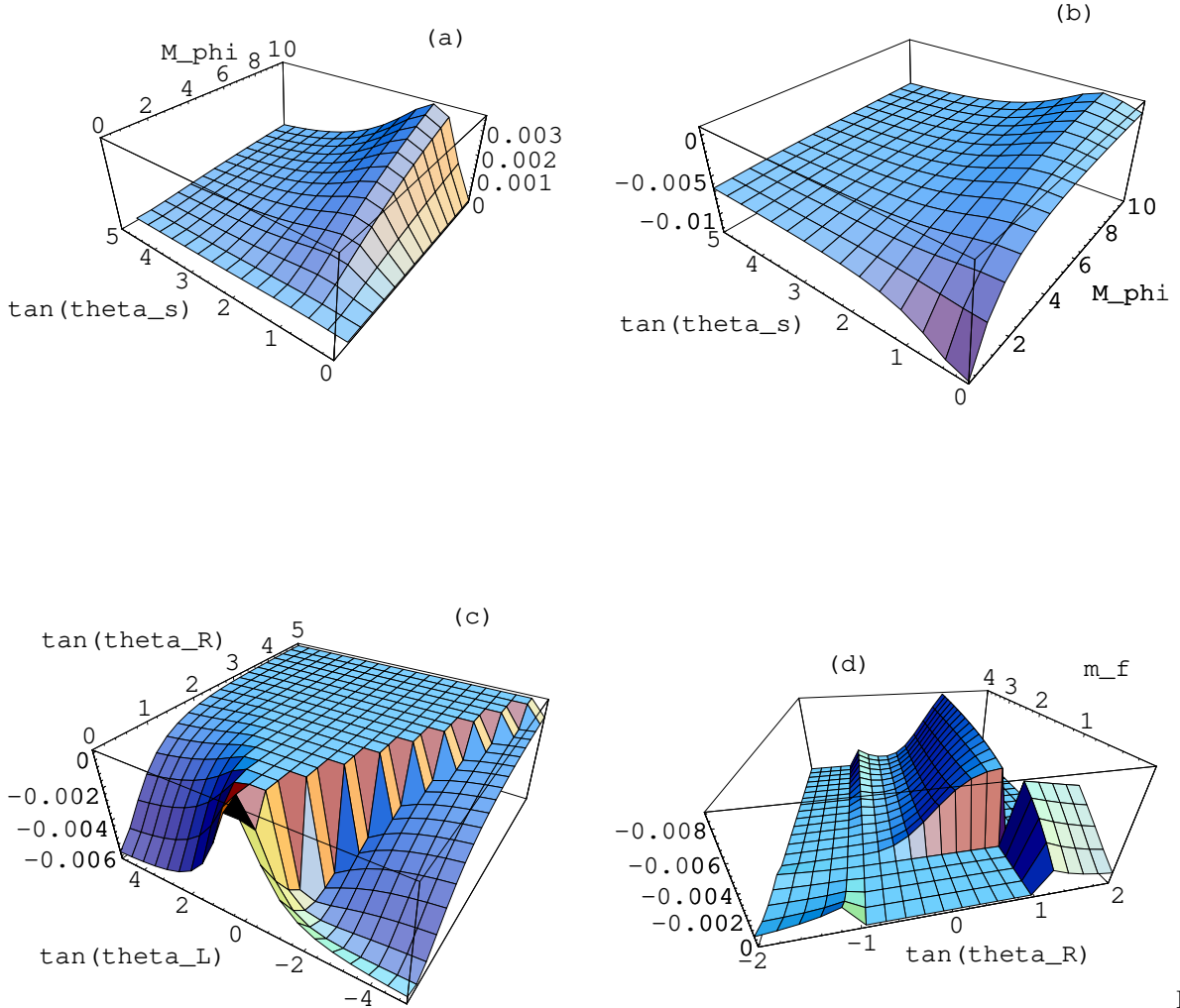


Fig-

ure 8: The dependence of  $g_L^b$  on the various supersymmetric parameters. Since  $g_L^b$  depends only on mass ratios in our approximation, the units of mass are arbitrary, with the masses of all the charginos and squarks which are not being varied set to unity.

One might therefore get the impression that it is easy to explain  $R_b$  using supersymmetric contributions to the  $Zb\bar{b}$  vertex. The problem is that to get a large enough contribution one is driven to a rather special region of parameter space, which comes close to satisfying condition (108). As mentioned above, the consequent condition (112) prevents one from making the chargino masses arbitrarily heavy. This, coupled with the suppression in  $R_b$  when the squarks are heavier than the charginos, means that all the relevant supersymmetric particles must be relatively light, except the charged Higgs which has to be heavy to suppress the wrong-sign contribution from  $H^+-t$  loops. Thus in the example of Fig. 8c, the preferred values of  $c_R = 1$ ,  $s_L = \pm 1$ ,  $s_R = c_L = 0$  imply that  $m_f = v \sin \beta$  and  $m_{f'} = v \cos \beta$ , while  $\mu \cong M_2 \cong 0$ , which are precisely the circumstances of the supersymmetric models considered in Refs. [27] and [28]. Fig. 8d, on the other hand, has its maximum value of  $R_b$  at  $c_R = s_R = c_L = -s_L = 1$ , implying  $\tan \beta = 1$  and thus from (112) that  $|m_{f'}| + |m_f| = 2M_W$ . Because the lightest chargino mass is constrained by experimental lower limits, there is little parameter space for getting a large hierarchy between the two chargino masses, as one would want in the present example in order to get the full shift of  $-0.0067$  in  $g_L^b$ . This seems to be the reason that Ref. [29] reaches a somewhat pessimistic conclusion about whether supersymmetry can solve the  $R_b$  problem: it is easy to miss the important region of the multi-dimensional parameter space when doing a random search by Monte Carlo sampling. In contrast, our analysis allows one to pinpoint just where the favorable regions are for solving the  $R_b$  problem.

We thus see that it is possible to understand many of the conclusions in the literature [27]–[31] on supersymmetry and  $R_b$  using some rather simple analytic formulas. These include the preference for small values of  $\tan \beta$  as well as light higgsinos and squarks.

## 6. Future Tests

If we exclude the possibility that the experimental value of  $R_b$  is simply a  $3.7\sigma$  statistical fluctuation, we can expect that, once the LEP collaborations have completed their analyses of all the data collected during the five years of running at the  $Z$  pole, the ‘ $R_b$  crisis’ will become an even more serious problem for the standard model. (Of course, it is wise to keep in mind that there may be a simple explanation, namely that some systematic uncertainties in the analysis of the experimental data are still not well understood or have been underestimated.) In sections 3-5 we have discussed a variety of models of new physics which could account for the experimental measurement of  $R_b$ . The next obvious step is to consider which other measurements may be used to reveal the presence of this new physics.

The most direct method of finding the new physics is clearly the discovery of new particles with the correct couplings to the  $Z$  and the  $b$  quark. However, failing that, there

are some indirect tests. For example, many of the new-physics mechanisms which have been analysed in this paper will affect the rate for some rare  $B$  decays in a predictable way. The rates for the rare decays  $B \rightarrow X_s \ell^+ \ell^-$  and  $B \rightarrow X_s \nu \bar{\nu}$  are essentially controlled by the  $Z\bar{b}s$  effective vertex  $\Gamma_{bs}^\mu$ , since additional contributions (such as box diagrams and  $Z\text{--}\gamma$  interference) are largely subleading.<sup>13</sup> In the SM, in the approximation made throughout this paper of neglecting the  $b$ -quark mass and momentum, a simple relation holds between the dominant  $m_t$  vertex effects in  $R_b$  and in the effective  $Z\bar{b}s$  vertex  $\Gamma_{bs}^\mu$ :

$$\Gamma_{bs}^{\mu, SM} = \frac{V_{tb}^* V_{ts}}{|V_{tb}|^2} \delta \Gamma^{\mu, SM} \quad (113)$$

where  $\delta \Gamma^{\mu, SM}$  is defined as in eq. (26) with the SM form factor as given in eqs. (27) and (38). The meaning of eq. (113) is that, within the SM, the  $Z\bar{b}s$  effective vertex measurable in  $Z$ -mediated  $B$  decays represents a *direct* measurement of the  $m_t$ -dependent vertex corrections contributing to  $R_b$ , modulo a ratio of the relevant CKM matrix elements. In particular, both corrections vanish in the  $m_t \rightarrow 0$  limit. The question is now: how is this relation affected by the new physics invoked in Secs. 3-5 to explain  $R_b$ ?

Consider first the tree-level  $b\text{--}b'$  mixing effects analysed in Sec. 3. It is straightforward to relate the corrections of the LH and RH  $Z\bar{b}b$  couplings to new tree-level mixing-induced FCNC couplings  $g_{L,R}^{bs}$ . In this case eq. (5) reads

$$g_{L,R}^{bs} = \sum_{\alpha w} (g_w^\alpha)_{L,R} \mathcal{U}_{L,R}^{\alpha b*} \mathcal{U}_{L,R}^{\alpha s} \mathcal{M}^{w1} . \quad (114)$$

Hence  $g_{L,R}^{bs}$  involve the same gauge couplings and mixing matrices that determine the *deviation* from the SM of the flavour-diagonal  $b$  couplings.

It is also true that, for many models of new physics, the loop corrections to the  $Z\bar{b}b$  vertex would change the effective  $Z\bar{b}s$  vertex in much the same way, therefore inducing computable modifications to the SM electroweak penguin diagrams. In these models, for each loop diagram involving the new states  $f, f'$  and their coupling to the  $b$ -quark  $g_{ff'b}$ , there will be a similar diagram contributing to  $\Gamma_{bs}^\mu$  that can be obtained by the simple replacement  $g_{ff'b} \rightarrow g_{ff's}$ . For example, the general analysis of  $t$ -quark mixing effects presented in Sec. 4 can be straightforwardly applied to  $Z$ -mediated  $B$  decays. Deviations from the SM predictions for the  $B \rightarrow X_s \ell^+ \ell^-$  and  $B \rightarrow X_s \nu \bar{\nu}$  decay rates can be easily

---

<sup>13</sup> Due to the absence of  $Z\text{--}\gamma$  interference and of large renormalization-group-induced QCD corrections, the process  $B \rightarrow X_s \nu \bar{\nu}$  represents theoretically the cleanest proof of the effective  $Z\bar{b}s$  vertex [32].

evaluated by means of a few simple replacements like  $|V_{tb}|^2 \rightarrow V_{tb}^* V_{ts}$  and  $|V_{t'b}|^2 \rightarrow V_{t'b}^* V_{t's}$  in all our equations.<sup>14</sup> To a large extent, this is also true for SUSY models. Indeed, the analysis of the SUSY contributions to the  $Z\bar{b}s$  form factor [34] can teach much about SUSY effects in  $R_b$ . And once a particular region of parameter space suitable to explain the  $R_b$  problem is chosen, a definite *numerical* prediction for the  $B \rightarrow X_s \ell^+ \ell^-$  and  $B \rightarrow X_s \nu \bar{\nu}$  decay rates can be made.

This brief discussion shows that, for a large class of new-physics models, the new contributions to  $R_b$  and to the effective  $\Gamma_{bs}^\mu$  vertex are computable in terms of the same set of new-physics parameters. Therefore, for all these models, the assumption that some new physics is responsible for the deviations of  $R_b$  from the SM prediction will imply a quantitative prediction of the corresponding deviations for  $Z$ -mediated  $B$  decays.

However, this statement cannot be applied to all new-physics possibilities. For example, if a new  $Z'$  boson is responsible for the measured value of  $R_b$ , then no signal can be expected in  $B$  decays, since in this case the new physics respects the GIM mechanism. This would also be true if  $m_b$ -dependent effects are responsible for the observed deviations in  $R_b$  as could happen, for example, in the very large  $\tan \beta$  region of multi-Higgs-doublet or SUSY models. More generally, the loop contributions of the new states  $f, f'$  can be different, since  $g_{ff's}$  is not necessarily related to  $g_{ff'b}$ , and in particular, whenever the new physics involved in  $R_b$  couples principally to the third generation, it is quite possible that no sizeable effect will show up in  $B$  decays. Still, the study of  $B \rightarrow X_s \ell^+ \ell^-$  and  $B \rightarrow X_s \nu \bar{\nu}$  could help to distinguish between models that do or do not significantly affect these decays.

Unfortunately, at present only upper limits have been set on the branching ratios for  $B \rightarrow X_s \ell^+ \ell^-$  [35]–[37] and  $B \rightarrow X_s \nu \bar{\nu}$  [32]. Since these limits are a few times larger than the SM predictions, they cannot help to pin down the correct solution to the  $R_b$  problem. However, future measurements of these rare decays at  $B$  factories could well confirm that new physics is affecting the rate of  $b$ -quark production in  $Z$  decays, as well as give some hints as to its identity. If no significant deviations from the SM expectations are detected, this would also help to restrict the remaining possibilities.

---

<sup>14</sup> For example, the particular case of mixing of the top-quark with a new isosinglet  $T'$ , and the corresponding effects induced on the  $Z\bar{b}s$  vertex, was studied in Ref. [33] through an analysis very similar to that of Sec. 4.

## 7. Conclusions

Until recently, the SM has enjoyed enormous success in explaining all electroweak phenomena. However, a number of chinks have started to appear in its armour. There are currently several disagreements between theory and experiment at the  $2\sigma$  level or greater. They are:  $R_b \equiv \Gamma_b/\Gamma_{\text{had}}$  ( $3.7\sigma$ ),  $R_c \equiv \Gamma_c/\Gamma_{\text{had}}$  ( $2.5\sigma$ ), the inconsistency between  $A_e^0$  as measured at LEP with that determined at SLC ( $2.4\sigma$ ), and  $A_{FB}^0(\tau)$  ( $2.0\sigma$ ). Taken together, the data now exclude the SM at the 98.8% confidence level.

Of the above discrepancies, it is essentially only  $R_b$  which causes problems. If  $R_b$  by itself is assumed to be accounted for by new physics, then the fit to the data despite the other discrepancies is reasonable ( $\chi_{\text{min}}^2/\text{d.o.f.} = 15.5/11$ ) – the other measurements could thus be regarded simply as statistical fluctuations.

In this paper we have performed a systematic survey of new-physics models in order to determine which features give corrections to  $R_b$  of the right sign and magnitude. The models considered can be separated into two broad classes: those in which new  $Z\bar{b}b$  couplings appear at tree level, by  $Z$  or  $b$ -quark mixing with new particles, and those which give loop corrections to the  $Z\bar{b}b$  vertex. The latter type includes  $t$ -quark mixing and models with new scalars and fermions. We did not consider technicolour models or new gauge bosons appearing in loops since these cases are much more model-dependent.

The new physics can modify either the left-handed (LH) or right-handed RH  $Z\bar{b}b$  couplings,  $g_L^b$  or  $g_R^b$ . To increase  $R_b$  to its experimental value,  $\delta g_L^b$  must be negative and have a magnitude typical of a loop correction with large Yukawa couplings. Thus  $\delta g_L^b$  could either be a small tree-level effect, or a large one-loop effect. On the other hand, the SM value of  $g_R^b$  is opposite in sign to its LH counterpart and is about five times smaller. Therefore one would need a large tree-level modification to  $g_R^b$  to explain for  $R_b$ .

Here are our results:

- (1) *Tree-level Effects*: It is straightforward to explain  $R_b$  if the  $Z$  or  $b$  mix with new particles. With  $Z$ – $Z'$  mixing there are constraints from neutral-current measurements, but these do not exclude all models. Using  $b$ – $b'$  mixing is easier since the experimental value of  $R_b$  can be accommodated by  $b_L$ – $b'_L$  or  $b_R$ – $b'_R$  mixing. If the mixing is in the LH  $b$  sector, then solutions are possible so long as  $I'_{3L} < -1/2$ . Additional possibilities with  $I'_{3L} > 0$  are phenomenologically and theoretically disfavored. For RH  $b$  mixing, if  $I'_{3R} > 0$  then small mixing is permitted, while if  $I'_{3R} < 0$ , large mixing is necessary. Interestingly, such large RH mixing angles are not ruled out phenomenologically. A number of papers in the literature have appealed to  $b$ – $b'$  mixing to explain  $R_b$ . Our “master formula” (8) and Table 2 include all of these models, as well as many others.

- (2) *Loops:  $t$ - $t'$  Mixing*: In the presence of  $t$ - $t'$  mixing, the SM radiative correction can be reduced, depending on the weak isospin quantum numbers of the  $t'$  as well as on the LH and RH mixing angles. However, we found that it is not possible to completely explain  $R_b$  via this method. The best we can do is to decrease the discrepancy between theory and experiment to about  $2\sigma$ . Such a scenario predicts the existence of a light ( $\sim 100$  GeV) charge  $2/3$  quark, decaying primarily to  $Wb$ .

- (3) *Loops: Diagonal Couplings to the  $Z$* : We considered models with exotic fermions and scalars coupling to both the  $Z$  and  $b$ -quark. We assumed that the couplings to the  $Z$  are diagonal, *i.e.* there are no flavour-changing neutral currents (FCNC's). The correction  $\delta g_L^b$  can then be written in a simple form, eq. (82). The key point is that  $\delta g_L^b$  is proportional to  $I_{3L}^f - I_{3R}^f$ , where  $I_{3L,R}^f$  is the third component of weak isospin of the fermion field  $f_{L,R}$  in the loop. This explains at a glance why many models, such as multi-Higgs-doublet models and Zee-type models, have difficulty explaining  $R_b$ . Since the dominant contributions in these models typically have top-type quarks ( $I'_{3L} = \frac{1}{2}$ ,  $I'_{3R} = 0$ ) circulating in the loop, they give corrections of the wrong sign to  $R_b$ . However, these considerations did permit us to construct viable models of this type which do explain  $R_b$ . Two such examples are given Sec. 5.4, and many others can be invented.

- (4) *Loops: Nondiagonal Couplings to the  $Z$* : We also examined models with exotic fermions and scalars which were allowed to have nondiagonal couplings to the  $Z$ . Such FCNC's can occur when particles of different weak isospin mix. The correction  $\delta g_L^b$  is much more complicated (eq. (86)) than in the previous case; even its sign is not obvious. However there are several interesting limiting cases where it again becomes transparent. The contributions to  $R_b$  of supersymmetry fall into this category, which we discussed in some detail.

## Acknowledgements

This research was financially supported by NSERC of Canada and FCAR du Québec. EN wishes to acknowledge the pleasant hospitality of the Physics Department at McGill University, during the final stage of this work. DL would like to thank Ken Ragan for helpful conversations.



## 8. References

- [1] LEP electroweak working group and the LEP collaborations, “A Combination of Preliminary LEP Electroweak Results and Constraints on the Standard Model”, prepared from summer 1995 conference talks.
- [2] SLC Collaboration, as presented at CERN by C. Baltay (June 1995).
- [3] CDF Collaboration, F. Abe *et.al.*, *Phys. Rev. Lett.* **74** (1995) 2626; D0 Collaboration, S. Abachi *et.al.*, *Phys. Rev. Lett.* **74** (1995) 2632.
- [4] C.P. Burgess, S. Godfrey, H. König, D. London and I. Maksymyk, *Phys. Rev.* **D49** (1994) 6115.
- [5] P. Bamert, C.P. Burgess and I. Maksymyk, *Phys. Lett.* **356B** (1995) 282.
- [6] P. Bamert, McGill University preprint McGill/95-64, hep-ph/9512445, (1995).
- [7] M.E. Peskin and T. Takeuchi, *Phys. Rev. Lett.* **65** (1990) 964; *Phys. Rev.* **D46** (1992) 381; W.J. Marciano and J.L. Rosner, *Phys. Rev. Lett.* **65** (1990) 2963; D.C. Kennedy and P. Langacker, *Phys. Rev. Lett.* **65** (1990) 2967; B. Holdom and J. Terning, *Phys. Lett.* **247B** (1990) 88.
- [8] M. Shifman, *Mod. Phys. Lett.* **A10**, (1995) 605; University of Minnesota preprint TPI-MINN-95/32-T, hep-ph/9511469 (1995).
- [9] P. Chiappetta, J. Layssac, F.M. Renard and C. Verzegnassi, Université de Montpellier preprint PM/96-05, hep-ph/9601306, 1996; G. Altarelli, N. Di Bartolomeo, F. Feruglio, R. Gatto and M.L. Mangano, CERN preprint CERN-TH/96-20, hep-ph/9601324, 1996.
- [10] C.-H.V. Chang, D. Chang and W.-Y. Keung, National Tsing-Hua University preprint NHCU-HEP-96-1, hep-ph/9601326, 1996.
- [11] J Bernabéu, A. Pich and A. Santamaría, *Phys. Lett.* **200B** (1988) 569. For other discussions of the radiative corrections to  $Z\bar{b}b$ , see A.A. Akhundov, D. Yu. Bardin and T. Riemann, *Nucl. Phys.* **B276** (1986) 1; W. Beenakker and W. Hollik, *Zeit. Phys.* **C40** (1988) 141; B.W. Lynn and R.G. Stuart, *Phys. Lett.* **252B** (1990) 676; J Bernabéu, A. Pich and A. Santamaría, *Nucl. Phys.* **B363** (1991) 326.

- [12] E. Ma, University of California at Riverside preprint UCRHEP-T153, hep-ph/9510289, 1995
- [13] T. Yoshikawa, Hiroshima University preprint HUPD-9528, hep-ph/9512251, 1995.
- [14] G. Bhattacharyya, G.C. Branco and W.-S. Hou, CERN preprint CERN-TH/95-326, hep-ph/9512239, 1995.
- [15] E. Nardi, E. Roulet and D. Tommasini, *Phys. Rev.* **D46** (1992) 3040.
- [16] B. Holdom, *Phys. Lett.* **351B** (1995) 279.
- [17] R. Stephens, plenary talk given at the II Rencontres du Vietnam.
- [18] See, for example, P. Langacker and D. London, *Phys. Rev.* **D38** (1988) 886.
- [19] E. Nardi, E. Roulet and D. Tommasini, *Nucl. Phys.* **B386** (1992) 239.
- [20] E. Nardi, E. Roulet and D. Tommasini, *Phys. Lett.* **344B** (1995) 225.
- [21] JADE Collaboration, E. Elsen et al., *Zeit. Phys.* **C46** (1990) 349.
- [22] CELLO Collaboration, H.J. Behrend et al., *Zeit. Phys.* **C4t** (1990) 333.
- [23] P. Bamert and C.P. Burgess, *Zeit. Phys.* **C66** (1995) 495 (hep-ph/9407203).
- [24] F. Abe et al. (CDF Collaboration), *Phys. Rev.* **D45** (1992) 3921.
- [25] E. Ma and D. Ng, *Phys. Rev.* **D53** (1996) 255.
- [26] L. Rolandi, H. Dijkstra, D. Strickland and G. Wilson, representing the ALEPH, DELPHI, L3 and OPAL collaborations, Joint Seminar on the First Results from LEP 1.5, CERN, Dec. 12th, 1995.
- [27] J.L. Feng, N. Polonsky and S. Thomas, SLAC preprint SLAC-PUB-95-7050, hep-ph/9511324.
- [28] E.H. Simmons and Y. Su, Boston University preprint, hep-ph/9602267.
- [29] J. Ellis, J.L. Lopez and D.V. Nanopoulos, CERN preprint CERN-TH/95-314, hep-ph/9512288.

- [30] J.D. Wells and G.L. Kane, SLAC preprint SLAC-PUB-7038, hep-ph/9510372.
- [31] Y. Yamada, K. Hagiwara and S. Matsumoto, KEK preprint KEK-TH-459, hep-ph/9512227.
- [32] Y. Grossmann, Z. Ligeti and E. Nardi, Weizmann Institute preprint WIS-95/49/Oct-PH, hep-ph/9510378, to appear in *Nucl. Phys.***B**.
- [33] E. Nardi, *Phys. Lett.* **365B** (1996) 327.
- [34] See, for example, S. Bertolini, F. Borzumati, A. Masiero and G. Ridolfi, *Nucl. Phys.* **B353** (1991) 591.
- [35] C. Albajar *et al.*, UA1 Collaboration, *Phys. Lett.* **262B** (1991) 63.
- [36] R. Balest *et al.*, CLEO Collaboration, Cornell preprint CLEO-CONF-94-4.
- [37] C. Anway-Wiese *et al.*, CDF Collaboration, Fermilab preprint Fermilab-Conf-95/201-E.

## 9. Figure Captions

- 1 A fit of the  $Z\bar{b}b$  couplings  $\delta g_{L,R}^b$  to  $Z$ -pole data from the 1995 Summer Conferences. The four solid lines respectively denote the  $1\sigma$ ,  $2\sigma$ ,  $3\sigma$ , and  $4\sigma$  error ellipsoids. The SM prediction lies at the origin,  $(0,0)$ . This fit yields  $\alpha_s(M_Z) = 0.101 \pm 0.007$ .
- 2 The experimentally allowed mixing angles for a mirror family. The thick line covers the entire area of values for  $s_L$  and  $s_R$  which are needed to agree with the experimental value for  $R_b$  to the  $2\sigma$  level or better. The thin line represents the one-parameter family of mixing angles which reproduce the SM prediction. Notice that the small-mixing solution, which passes through  $s_L = s_R = 0$ , is ruled out since  $I'_L = 0$  implies that any LH mixing will *reduce*  $g_L^b$  and thus increases the discrepancy with experiment.
- 3 The Feynman diagrams through which the top quark contributes to the  $Z\bar{b}b$  vertex within the Standard Model.
- 4 The additional Feynman diagrams which are required for models in which the  $t$  quark mixes with an exotic, heavy  $t'$  quark.
- 5 The one-loop vertex correction and self-energy contributions to the  $Z\bar{b}b$  vertex due to fermion-scalar loops.
- 6 The one-loop contributions to the  $Z\bar{b}b$  vertex due to the gauge-boson vacuum polarizations.
- 7 From top to bottom, the functions  $\mathcal{F}(m_f^2/M_\phi^2)$ ,  $F_R(r) = F_S(r)$  and  $F_L(r)$  which appear in the loop contribution to the left-handed  $Z\bar{b}b$  vertex, sections 5.1 and 5.3.
- 8 The dependence of  $g_L^b$  on the various supersymmetric parameters.